SAND84-1021
Unlimited Release
Printed July 1984

Distribution
UC-94E

# FINITE ELEMENT STUDY OF WORKING LEVEL SEPARATION AT THE WEEKS ISLAND SALT DOME

Dale S. Preece
Raymond D. Krieg
Applied Mechanics Division 1521
Sandia National Laboratories
Albuquerque, New Mexico 8'7185

## ABSTRACT

The Weeks Island salt dome has a former two-level room-and-pillar salt mine which is now filled with oil as part of the Strategic Petroleum Reserve (SPR). This study is a determination of the safe separation of the SPR level from a postulated outburst beneath it. A series of finite element structural analyses model the mine excavation, filling, outburst occurrence, and subsequent time until the year 2045 for various postulated separation distances. It is found that if the outburst is 100 ft or more from the SPR, then there is no discernable effect on the SPR. If the outburst is only 50 ft below the SPR, then there is a discernable but nonthreatening effect.

ACKNOWLEDGMENT

The authors would like to acknowledge Joel Miller and James K. Linn for very thorough reviews of this report.

CONTENTS

## FIGURES

TABLES

## SUMMARY

The Strategic Petroleum Reserve (SPR) caverns at Weeks Island salt dome consist of two levels of a room and pillar mine, formerly a salt mine. At some distance below the SPR, another salt mine is to be built. If a tall gas pocket were present between the mine and the SPR, and if it were breeched during mining, this resulting outburst might jeopardize the isolation of the SPR and endanger the mine below. In this study, a safe SPR-to-outburst separation distance is determined. Because of the creeping nature of the salt, the time dependent loading around the SPR outburst is modeled in some detail. The analysis follows the mine construction of the second level from 1955 and the SPR oil fill from 1980 to 1982. A pocket filled with gas at lithostatic pressure is postulated to be present throughout this time. New mining operations below the SPR are then postulated to breech the pocket creating a tall, 50 ft diameter cylindrical outburst which extends upward toward the SPR. This is assumed to take place in 1987. The structural response is followed until the year 2045. Separation distances between the outburst and SPR of 50, 100, 150, 250, and 350 ft are considered. A cylinder of salt 5000 ft in diameter and 3000 ft deep containing the SPR and outburst is included in the model. An initial depth dependent hydrostatic stress state is used together with body forces in the salt to model gravity effects. Salt is modeled as an elastic-secondary creep material. The study concludes with the clean result that with 100 ft or larger separation, there is no discernable effect on the SPR due to the outburst below. At 50 ft separation, there is a discernable but non-threatening effect. These results were indicated both by creep strains in the year 2045 and by Von Mises stresses for all time considered. Salt failure was studied with two failure models and indicated failure nowhere at any time. The probability of the postulated large outburst occurring at Weeks Island is not addressed in this report.

# FINITE ELEMENT STUDY OF WORKING LEVEL SEPARATION AT THE WEEKS ISLAND SALT DOME

## Problem Description

The Weeks Island salt dome is located south of New Iberia, Louisiana in the south central part of the state. It is described by Ortiz [1] from which the following is extracted. The "island" rises up to 170 feet above the surrounding marshland and is about two miles in diameter. The intracoastal waterway passes along the west edge of the "island." The dome has no caprock. A few feet of clay overlies the salt above which is 100-200 feet of sand and sediment. The dome is roughly 2 miles in diameter at 800 ft depth, 2 1/4 miles in diameter at 10,000 ft, and extends down to roughly 15,000 ft. Domal shale or sheath encircles the dome.

Rock salt mining production began in 1902 with a room and pillar operation at the first level (-535 MSL)(feet below Mean Sea Level). Production from the second level (-735 MSL) began in 1955. Pillars of the second level are nearly directly under the pillars of the first level. As mining extended to the east of the upper level, the room width increased from 50 to 70 feet with pillars remaining 100 feet in length and width throughout. Room heights are roughly 75 feet.

The Department of Energy has purchased a portion of the Weeks Island Mine including the two mined levels mentioned above for the Strategic Petroleum Reserve (SPR) program. These drifts have now been filled with crude oil. Because the volume used by the SPR is only a small part of the dome, it is reasonable to continue mining rock salt in other regions of the dome. The present study addresses the question of how far below the SPR storage area must a new working horizon be located in order to assure safe operation. The approach here is to use modern computationally based structural mechanics methods to calculate the expected behavior of the dome beginning with the mine opening at the lower level in 1955.

A dominant factor in the problem of vertical spacing between working levels is the presence of pockets of trapped gas. If these pockets are unexpectedly pierced by mining operations, the gas is released almost explosively. The resulting outburst generally is conical in shape with the large end toward the working drift. Outbursts in the Weeks Island mine have generally been small. In the lower level 38 blowouts under 10 ft in diameter were encountered, five were 10–20 ft in diameter, and three over 20 ft [1]. The largest was about 30 ft in maximum extent. Consequently, there is concern about the effect of encountering such a large gas pocket if one were to exist in the salt between the SPR lower level and a working horizon beneath. If a large gas pocket were penetrated by mining operations on the working horizon, the resulting outburst might weaken the SPR horizon if it were too near. Men and investments in the mine below might then be endangered. In the present study, we postulate a very large outburst and find the effect on the SPR horizon.

The size of the largest outburst which might possibly be found is not to be discussed here. Instead, we will consider encountering a hypothetical worst case gas pocket at the outset. This is postulated to result in a tall cylindrical outburst, 50 feet in diameter. The outburst would extend downward from the SPR and of course originate at the working horizon below. We assume that the pocket is initially filled with gas at lithostatic pressure. After outburst, the cylinder is further assumed to be occupied with no material which would support any forces, i.e., it is hollow. Studies similar to this were made by Henderson [2] in 1977 and Hilton, Benzley, and Gubbels [3] in 1979. There appear to be no fundamental errors in their work, but the state of the art has improved somewhat since then so it seems prudent to take a fresh look at the problem.

The Weeks Island SPR is shown schematically in Figure 1. The first level (at − 535 MSL) was mined over the years 1902-1955. The second level (at − 735 MSL) was mined over the years 1955 − 1975. The mine was filled with crude oil over the two year span of time ending in 1982. We assume that mining would begin below the SPR horizon sometime later and that a gas pocket would be encountered in 1987, producing a tall cylindrical outburst. We further assume that no effort would be made to repressurize or shore up

the outburst area. The large postulated outburst could occur at any time during the working life of the new postulated mine level. It was felt that the worst case was an outburst early in the life of the mine when little extraction had been completed. The compliant behavior around a mined horizon would cause some bridging across the horizon and result in slightly lower stresses around the outburst and SPR. The new mine horizon then was omitted entirely in the model. The behavior of the salt around the SPR near the outburst is then observed for the expected useful life of the SPR and beyond. The year 2045 is chosen here for the term and date in this study.

Several postulated distances from the outburst to the SPR lower horizon are considered: 350, 250, 150, 100, and 50 feet. For all these cases, we assume the outburst is directly beneath a room in the SPR. For the nearest outburst, we also consider the case where the outburst is directly beneath a pillar.

The model used to represent the problem, results of the analyses, and our conclusions are presented in the remainder of the report. Details of the model and more detailed results are contained in Appendix A. These details are included for the benefit of structural engineering specialists but are not necessary for understanding the important aspects of the analyses. Appendix B has been included to aid a person without an engineering background to understand the definition of some of the terms used in the body of the report.

## Model Description

Because of the general nature of this problem and our focused attention on the gas pocket area, it is prudent to use an axisymmetric representation of the problem as shown in Figure 2. The widths and heights of the rooms in the model are chosen to approximate the mine of Figure 1. The support areas of the pillars are also taken to be the same in the model as in the mine. Note that the first or upper level of the SPR has been omitted in the model. This has been done as a worst case since its presence would only tend to relieve pressure on the lower level. The postulated cylindrical outburst is

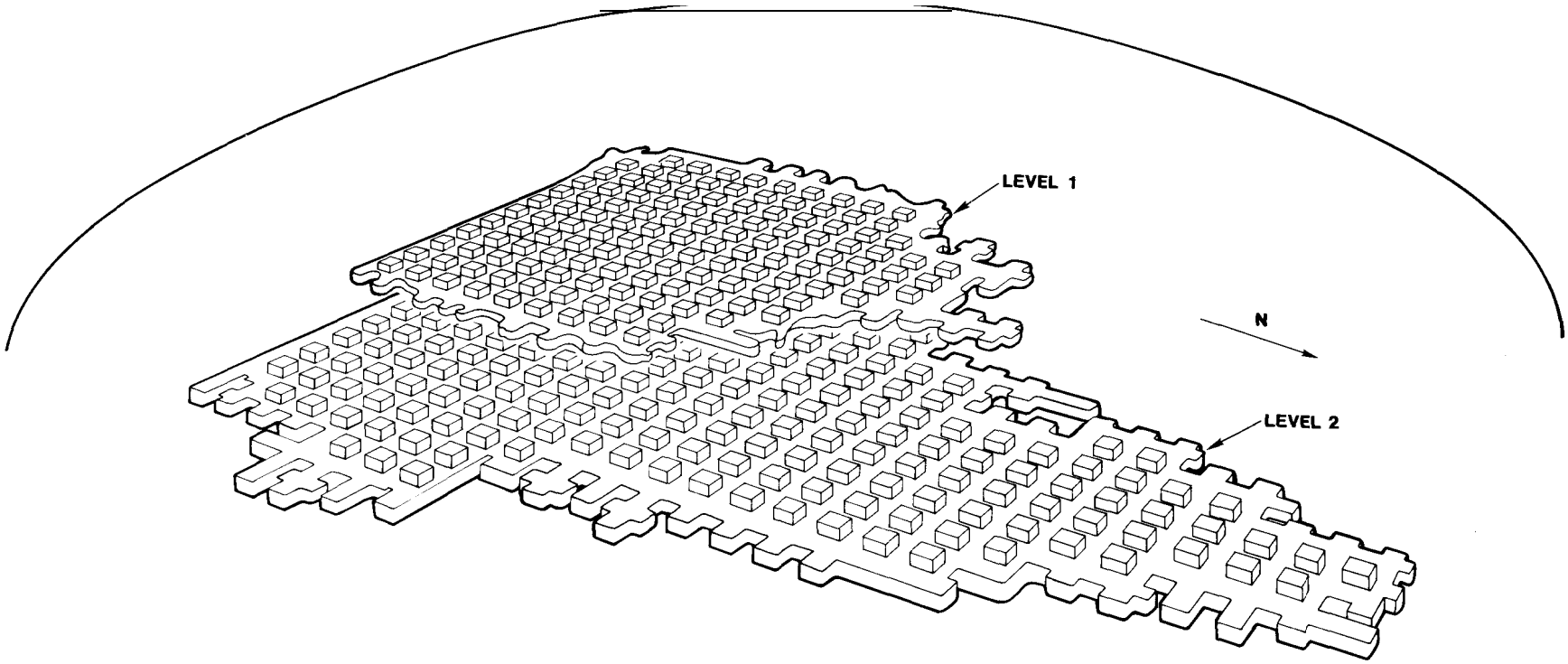


Figure 1 Schematic drawing of the two SPR levels in the Weeks Is and salt dome.

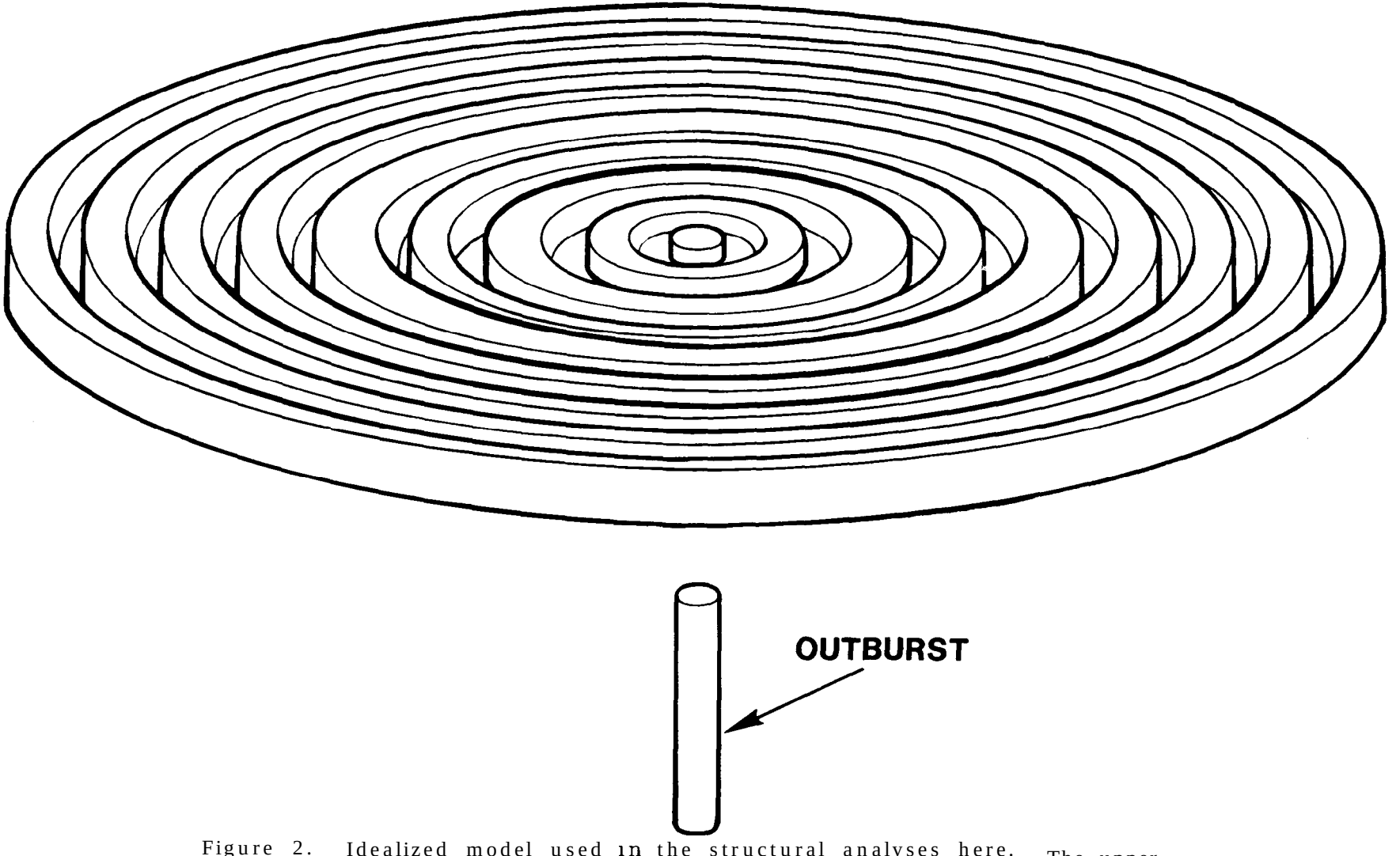


Figure 2. Idealized model used in the structural analyses here. The upper horizon has been omitted for simplicity.

pictured beneath the center of the SPR horizon in Figure 2. The lower extremity of the outburst would, of course, terminate at the assumed working level beneath the SPR. The postulated outburst is equally likely to occur at any time during the working life of the mine so that the working level could have various lateral extents. Since this level is to be no closer than 300 feet beneath the SPR, it was felt, based on earlier studies [3], that its effect would be minimal and hence is not included in the model here.

The history and postulated chronology of events are given in Table 1. Although it is tempting to omit all events prior to 1987, we felt a detailed history in the vicinity of the gas pocket was necessary in order to establish the correct stress field at the time of the outburst. Salt is a creeping or time dependent medium; the extent of a local disturbance spreads out with time.

There were six geometrically different cases analyzed in the study. The first five have the outburst directly beneath a room intersection in the SPR. These differ only in the separation distance between the top of the outburst and the SPR horizon. Distances of 350, 250, 150, 100, and 50 feet were used. The sixth case was also analyzed with 50 foot separation but with the outburst located beneath a pillar. In all cases, the outburst was modeled as a long 50 foot diameter cylinder. The lower extremity of the outburst was felt to be of little consequence so it was terminated 650 feet beneath the SPR horizon for convenience in each case.

The gas pocket prior to outburst was assumed to be filled with gas at lithostatic pressure. For convenience, this was chosen to be 1 psi per foot of depth in all cases. At the time of outburst, the pressure was suddenly reduced to zero. Further, it was assumed that no attempt would be made to fill the outburst volume and that the outburst would exist for 58 years as an unreinforced opening beneath the SPR mine. This should be well beyond the expected need for the SPR.

Table 1. History and Assumed Chronology of Events in the Modeled Scenario

| Time of Event | Description of Event | Days From Zero | Notes |
|---|---|---|---|
| 1902 | Upper level mining begins | - - - | Not included in model as worst case. |
| 1955 | Lower level mining beg ins | 0 | Modeled by decreasing pressure in the drifts until zero pressure is reached. |
| 1975 | Lower level mining ends | 7300 | |
| 1980 | Lower level begins filling with oil | 9125 | Modeled by increasing pressure in drifts until full oil density is reached. |
| 1982 | SPR fill complete | 9855 | |
| 1987 | Outburst occurs in mining beneath SPR | 11775 | Pressure in the cylindrical region is suddenly reduced from lithostatic to zero and no repairs are made. |
| 2045 | Problem extreme time | 33000 | |

## Numerical Method of Solution

The solution method applied here is the non-linear quasi-static finite element computer program (or code) SANCHO [4,5]. This code was written especially for solution of geomechanics problems in rock salt although it can be applied to a wide range of problems.

In this problem, we solve a set of differential equations and boundary conditions which govern the physics of the problem. Lithostatic initial stresses which vary with depth, internal pressure in the gas pocket, and pressure in the SPR horizon (due to the weight of the oil) are some of the forces which are included.

An elastic-secondary creep description of the rock salt is used. This description is based on an extensive set of laboratory tests on rock salt [6,7]. Comparison of salt from various sites shows only slight differences [8]. Short time triaxial compressive tests [9] were compared with similar tests from other Louisiana salt domes. The salt was found to be more variable with a slightly lower average strength. No creep tests were made on this particular salt but based on considerable experience base of geomechanisists at Sandia [6,8], the Weeks Island salt was judged to have roughly the same creep properties as that from West Hackberry. The details on salt properties which were used are given in Appendix A.

The problems as stated have exact solutions, but just as the mathematical quantity pi cannot be stated exactly in decimal form, we cannot find the exact solution to our problem. The finite element (FE) method has been developed by researchers in the applied mechanics community, principally in this country, to solve a wide range of problems. In the FE method, the region of the problem is discretized into a multitude of "elements" over which approximate solutions are determined. Theorems have been proven which state that the exact solution is approached as the number of elements grows. The finer the FE gridwork (or mesh) in the model, the better the approximation to the solution. However, the more elements there are in the model, the more expensive the computer solution becomes.

In Figure 3, the finite element gridwork is displayed on one half the region and the region boundaries simply displayed on the other half. A separation distance of 100 feet between the SPR and the top of a postulated outbrus t is displayed here. Note that no discretization is used in the circumferential direction since this is automatically accounted for in the axisymmetric solution algorithm used in SANCHO. In the various cases, we have used 1991 to 2327 elements.

SANCHO has been exercised on many rock salt problems associated with domal salt, the SPR [10,11,12] and the Waste Isolation Pilot Plant (WIPP) project in bedded salt [13,14,15]. In the Benchmark II study [16], SANCHO was compared with eight other codes. Results from SANCHO compare favorably with the other codes. Wawersik, et al [17] in another study, showed that computations agreed well with eight year mine closure data from Canada. In the present study, a check on our computations is provided because creep displacements in the lower level were measured prior to filling with oil. Ortiz [1] found that the floor to ceiling distance was decreasing at a rate of 0.5 inches per year. This closure rate appears to have been averaged data taken between 1961 and 1987 in Room 1 of the lower level [21]. This room is a 25 ft high drift along the west periphery of the mine. Being on the outer edge of the mine will result in lower closure. If the lower horizon rooms and pillars were all scaled by the factor of three seen in the measured room and actual SPR rooms, then the displacement in the 75 ft room would be 1.50 in/year. Computation of the slope of the closure curve in Figure 4 gives a maximum closure rate of 1.54 inches per year in 1976 when the mine was simulated to be at atmospheric pressure. Thus, the measured and predicted closure rates are relatively close.

To run each case required roughly 5000 seconds of central processor time on the CRAY 1S, one of the world's fastest computers.

## Results of Analyses

In the FE method, the solution for all stresses, forces, strains, and displacements are computed at all locations and at all times. We have chosen to display only the most pertinent of these results. Our objective

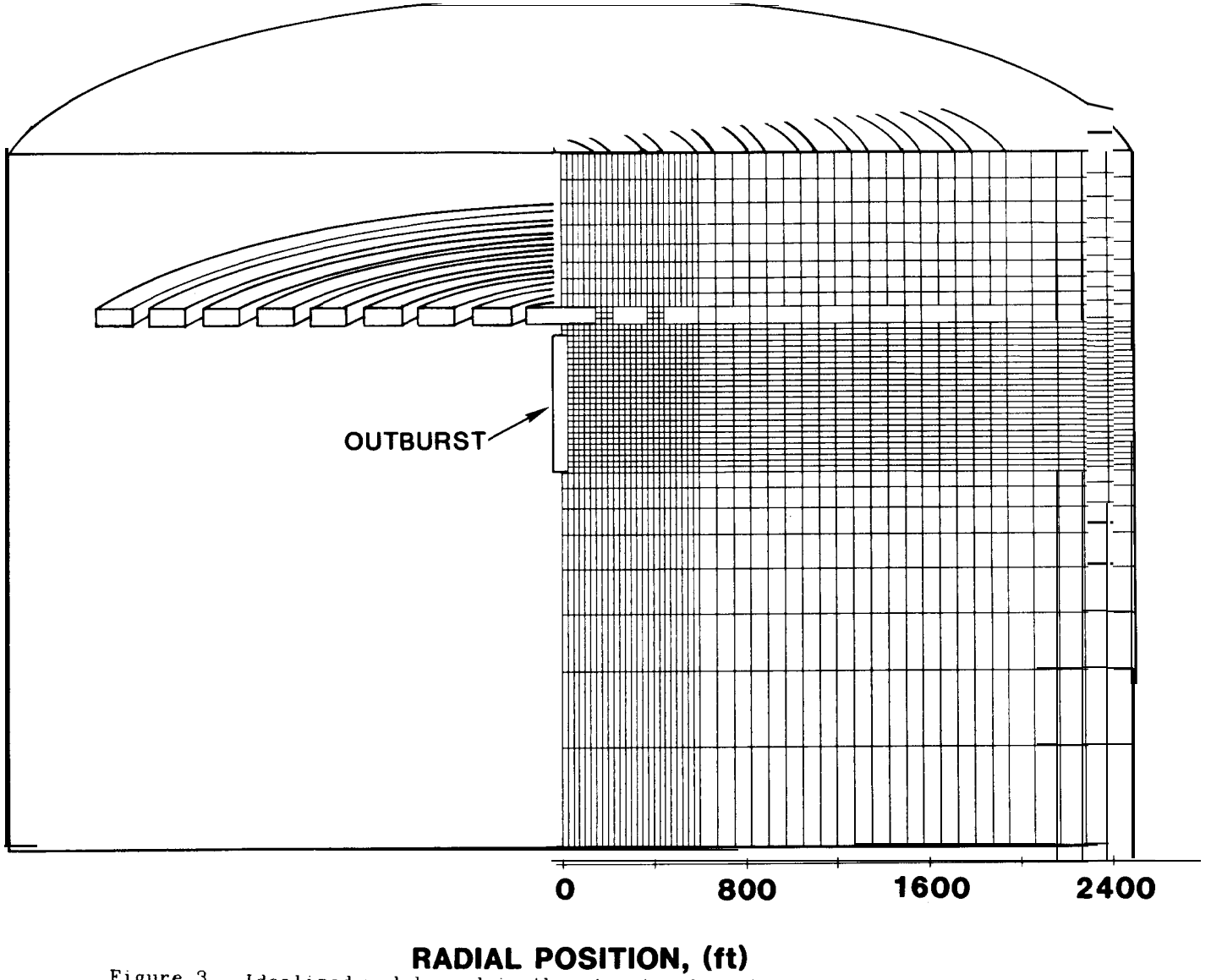


Figure 3. Idealized model used in the structural analyses, shown with the finite element grid superimposed on half the model. The case of a postulated outburst centered 50 ft beneath a room is shown.

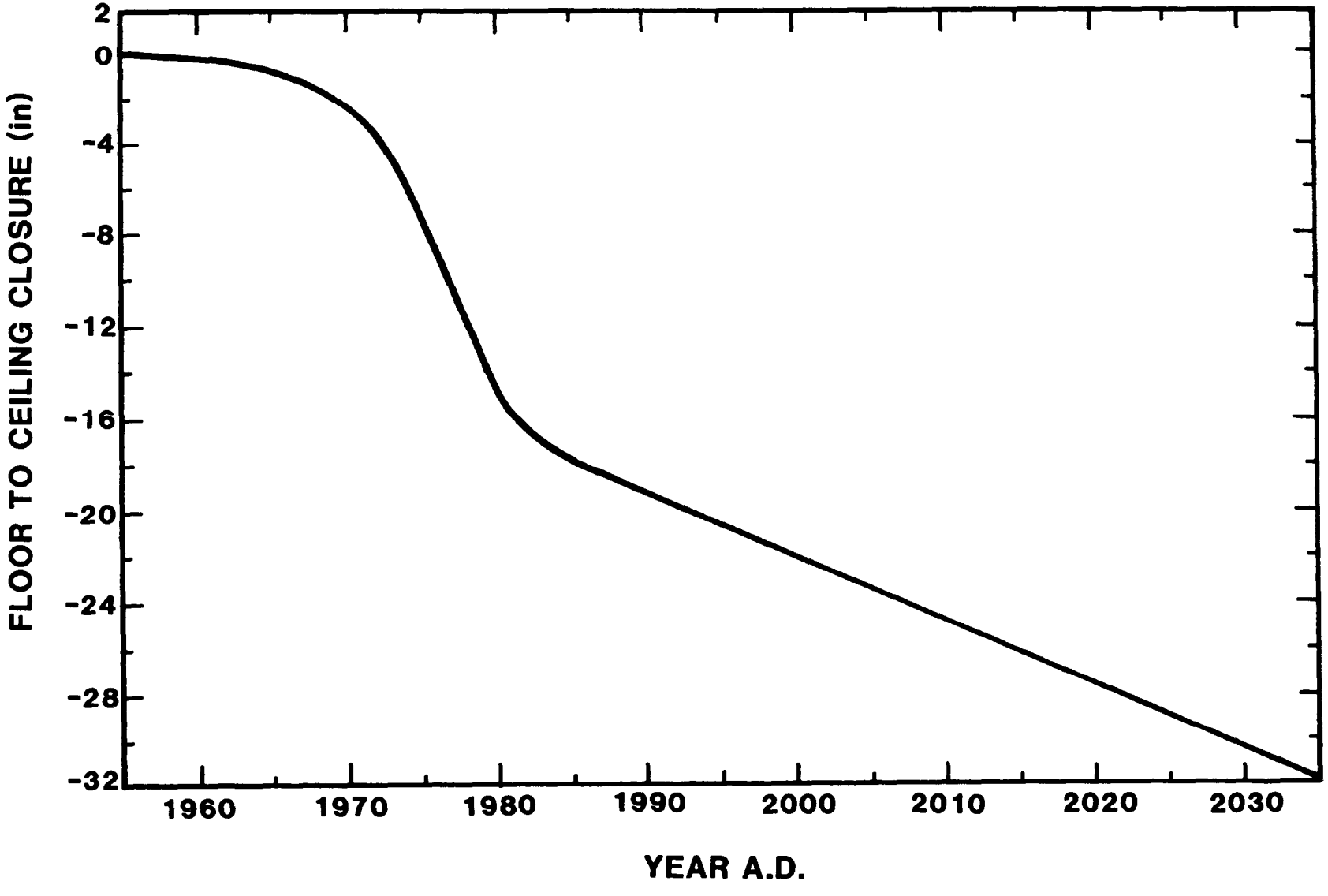


Figure 4. History of a computed floor-to-celling closure of the lower level SPR room at the centerline above a postulated outburst for various cases of outburst location.

is to use the results of these analyses to determine the minimum safe separation distance to a working horizon beneath the SPR. Recall that this was defined in our problem description as the minimum safe separation distance of the SPR from an outburst through which oil might be channeled into the working horizon below. We will consider how the most meaningful measures of displacement, strain, and stress around the SPR are disturbed by the presence of the outburst.

The most straightforward comparison we can make is to consider the floor-to-ceiling closure. In Figure 4, we see the history of the closure plotted for the case with a 50 ft separation between the outburst and the SPR horizon where the outburst is beneath a pillar. Note that there is no discernable disturbance in 1987 when an outburst is postulated to occur.

The closure for cases with other SPR-to-outburst separation distances were also plotted and compared with Figure 4. These plots (not given in the report because of similarity to Figure 4) show the same behavior, which implies that the immediate closure response in the SPR horizon would not be discernable if an outburst occurred, even as near as 50 ft away.

The Von Mises stress (as discussed in Appendix B) is associated with a tendency for a material to creep or deform in a time dependent manner, even when the loads are fixed. Figure 5a is a plot of lines of constant Von Mises stress superimposed on a cutaway of the SPR immediately before a postulated outburst. Figure 5b is a plot of the same cutaway immediately after the outburst. These are for the case where the postulated outburst is only 50 ft below a room in the SPR horizon. This pair of plots is a particularly effective display of the distribution of the stress disturbance. It shows only minor changes in the stress field around the SPR although stresses around the outburst are apparent. Figures 6a and 6b are similar plots for the case where the outburst is centered 50 ft beneath a pillar rather than a room. As before, the plots correspond to times immediately before and after the outburst. The stress distribution is qualitatively the same as the previous case. The outburst again appears to have only a minor effect on the stress distribution around the SPR.

For a ductile material such as rock salt, the Von Mises stress is the most meaningful stress in considering material failure. Two different failure criteria were considered in this study. These are discussed in Appendix A. In no case was "failure" of the salt ever indicated.

In this study, we focus our attention on the area between the top of the outburst and the bottom of the SPR. From Figures 5 and 6, the Von Mises stress in this area is as high on the centerline as anywhere in that area. Figure 7 is based on that observation. It summarizes the pertinent information regarding the Von Mises stress. The maximum value of the Von Mises stress on the centerline was found for a given case at a given time. This was then done for all times after 1987. All of these were then examined to find the largest Von Mises stress for this case for all time. This maximum over space and time will be called a maxi-max value and appears as one point in Figure 7. This was repeated for all cases. The 50 ft separation case was run with both a course and a fine mesh around the outburst/SPR area and with the outburst beneath a pillar rather than a room. These three calculations gave consistent results. Note that the stress magnitudes for all cases shown are very low. Von Mises stresses of roughly 140,000 psf or greater must be applied in several month-long laboratory tests for creep rates to be measured. Figure 7, however, clearly shows that the outburst has some effect on the Von Mises stress if the separation distance is only 50 ft but no effect for separation distances of 100 ft or more.

Another measure which must be examined is the creep strain. In Figure 8, lines of constant creep strain are superimposed on a cutaway of the SPR. These are predicted values in the year 2045 given that an outburst occurs beneath the SPR in 1987. Figure 9 is a similar plot for the postulated case of an outburst beneath a pillar rather than a room. In these figures, we note the rather modest strains in the area between the top of the outburst and bottom of the SPR, even for cases of 50 ft separation.

For any given case, the creep strains in the year 2045 can be searched along the centerline between the SPR and the outburst to find the maximum

value. This value is plotted in Figure 10 for each SPR-to-outburst separation distance considered. From this plot, we see a similar resultto that seen in the Von Mises plot in Figure 7. The creep strains are extremely small for all cases. There is some effect of the outburst on the creep of the SPR room for a 50 ft separation distance but no effect for separation distances of 100 ft or more.

## Conclusions

Three quantities have been examined in order to decide on an acceptable separation distance between the top of an outburst and the floor of the lower level SPR horizon at Weeks Island. The first was to examine the effect on closure of the SPR when the postulated outburst occurs. The results showed that there was essentially no effect even for the 50 ft separat ion cases. The second quantity considered was the maximum Von Mises stress in time and space along the centerline between the SPR horizon and the postulated outburst. The result in Figure 7 shows that even at 50 ft separation distance, the maxi-max Von Mises stress is not excessive. The third quantity examined was the accumulated maximum creep strain on the centerline between the SPR and the postulated outburst. In the year 2045, the creep strains are still more than an order of magnitude lower than the creep strain level which would cause concern, even for the 50 ft separation distance. A fourth quantity which was mentioned in passing was a failure measure for salt. There are two which were applied, but both showed failure to be so remote that the applicability of the measures became questionable. They simply show that salt failure is not a concern here.

One could probably justify the safety of a working mine beneath the SPR such that the top of an outburst 50 ft away from the SPR would be allowed. However, it appears that if a 100 ft separation is maintained, then we calculate that there is no measurable effect on the SPR whatsoever. Unfortunately, one cannot know with certainty whether any outburst larger than the 30 ft maximum encountered in level 2 would be found when mining below the SPR or what size the largest outburst would be. The final decision of a safe distance to a working horizon below the SPR must involve both an estimate of possible outbursts and the results of this study.

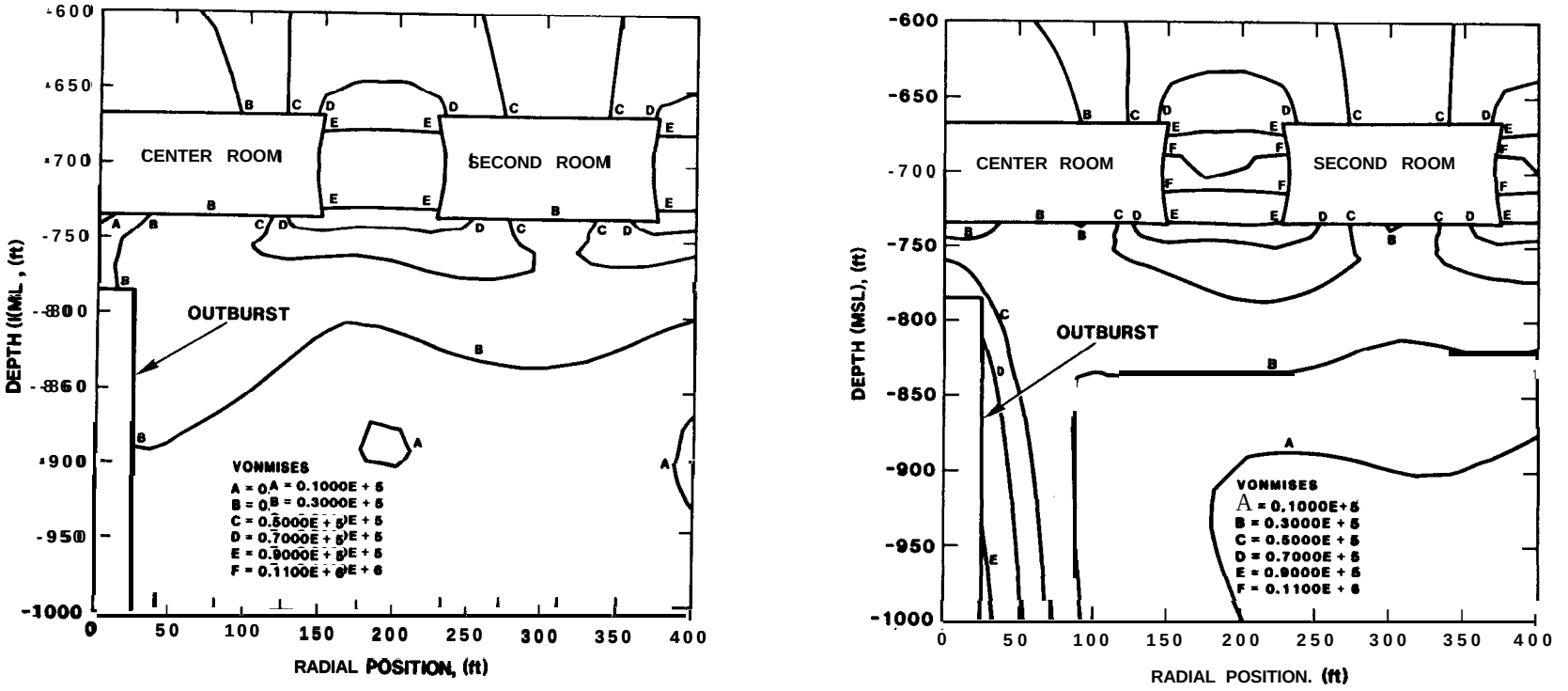


Figure 5. Contours of constant Von Mises stress (psf) superimposed on the model The entire model was used in the analysis, but only the region near the top of the outburst is shown. Results immediately before and after the outburst are shown at left and right, respectively. The outburst is postulated to be 50 ft beneath a room in the SPR.

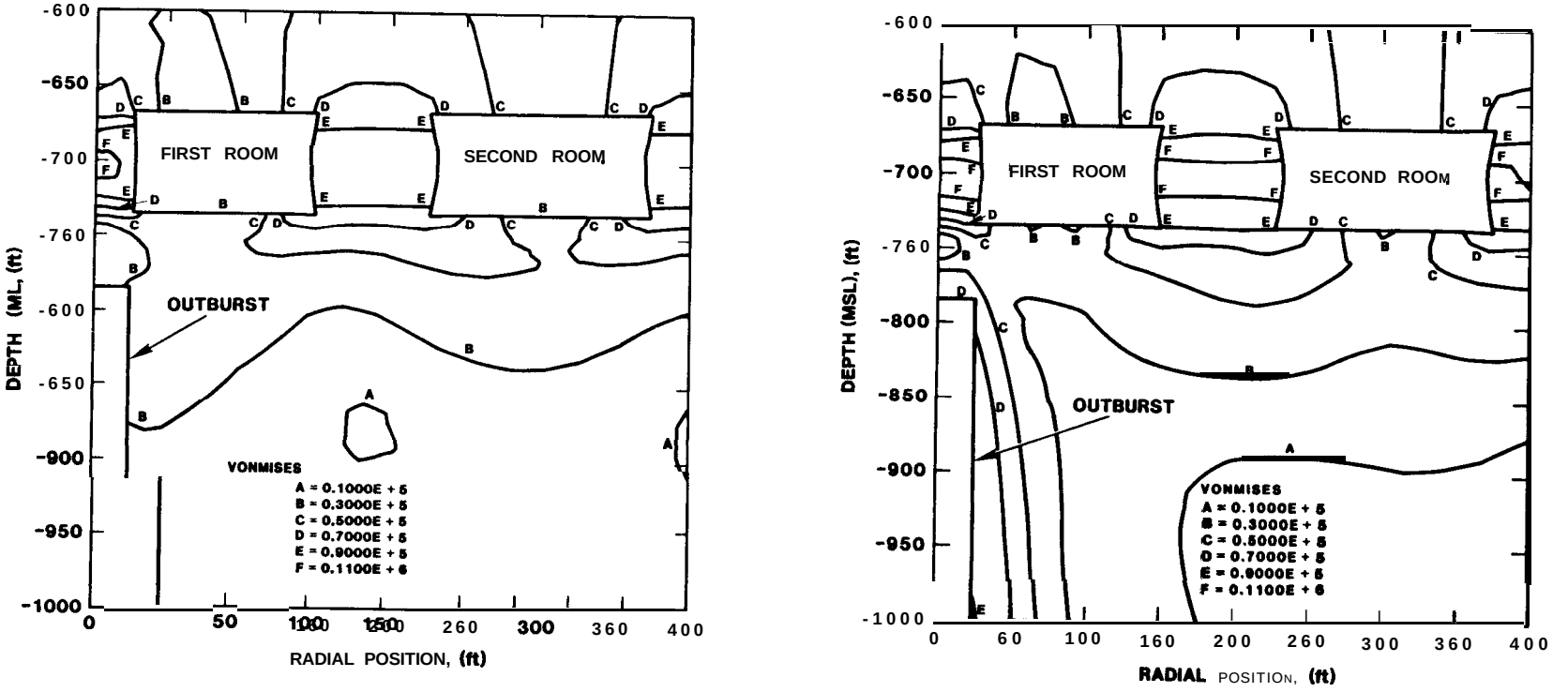


Figure 6. Contours of constant Von Mises stress (psf) superimposed on the model The entire model was used in the analysis but only the region near the top of the outburst is shown. Results immediately before and after the outburst are shown at left and right, respectively. The outburst is postulated to be 50 ft beneath a pillar in the SPR.

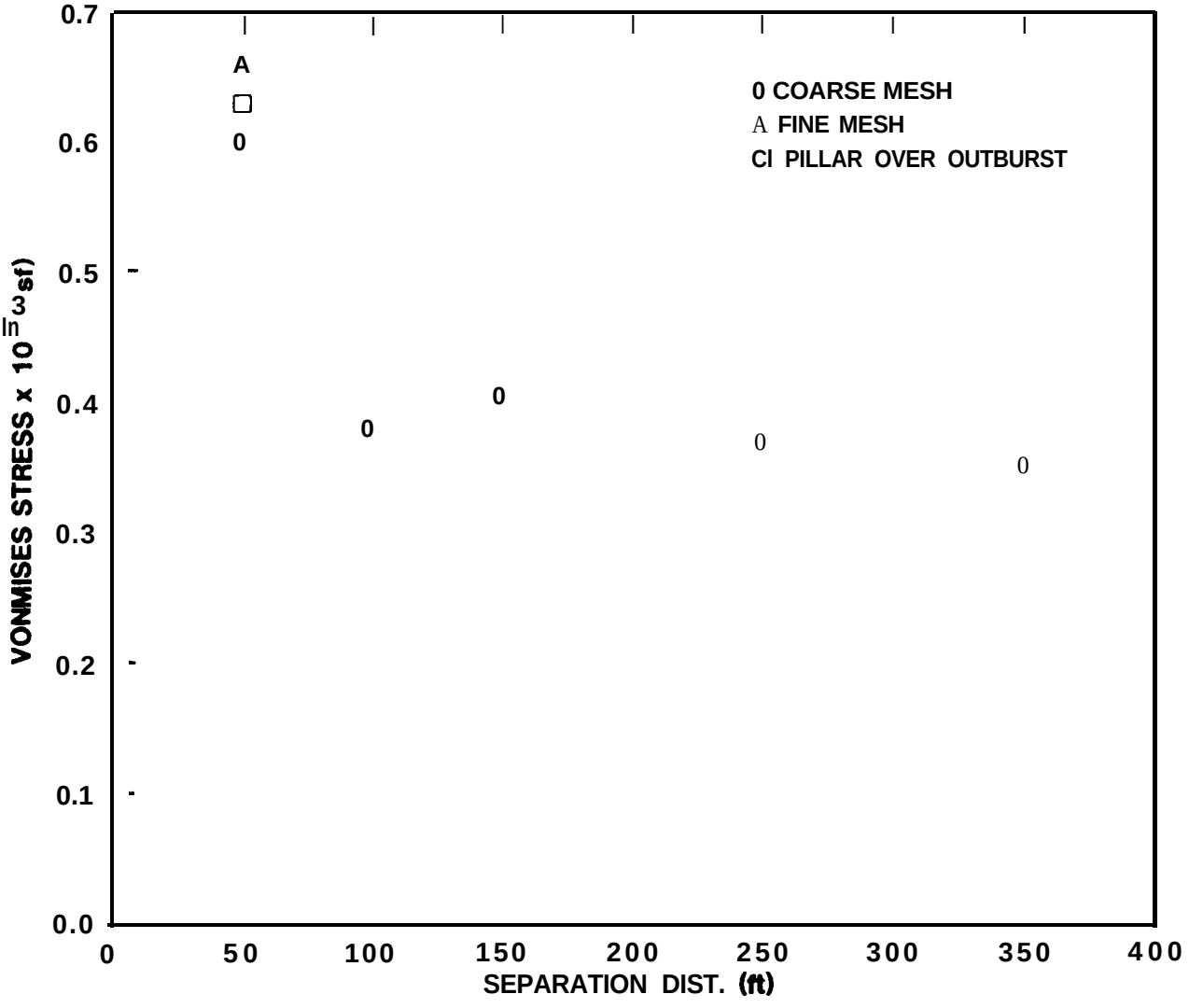


Figure 7. Maximum value of Von Mises stress on the centerline between the SPR horizon and the top of the postulated outburst and also maximum for all time after 1987 plotted for the seven cases as a function of separation distance between the SPR horizon and the top of the outburst.

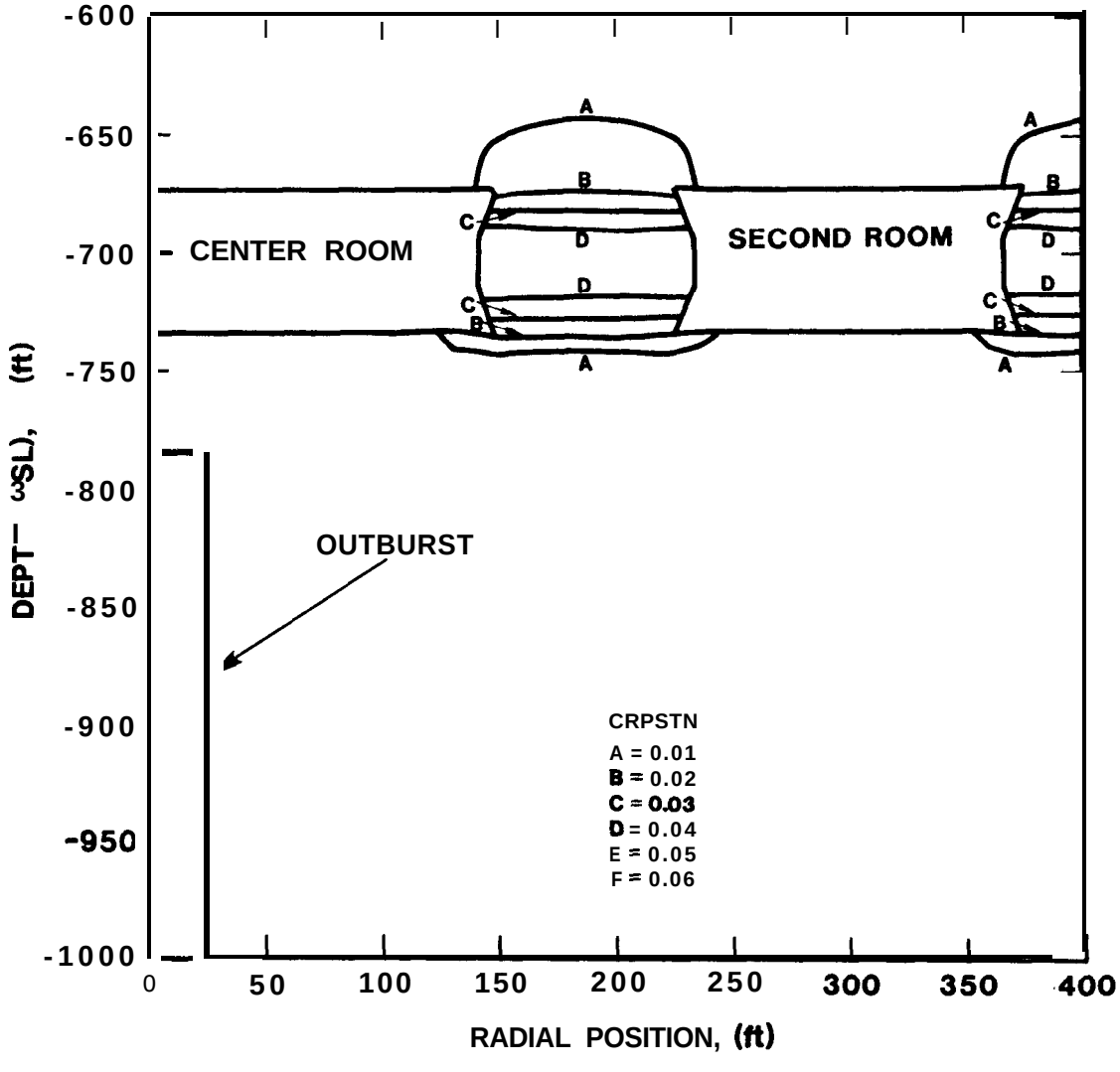


Figure 8. Contours of constant creep strain in the year 2045 assuming an outburst beneath the SPR occurs in the year 1987 due to mining below. The top of the outburst is assumed to be 50 ft beneath a room in the SPR.

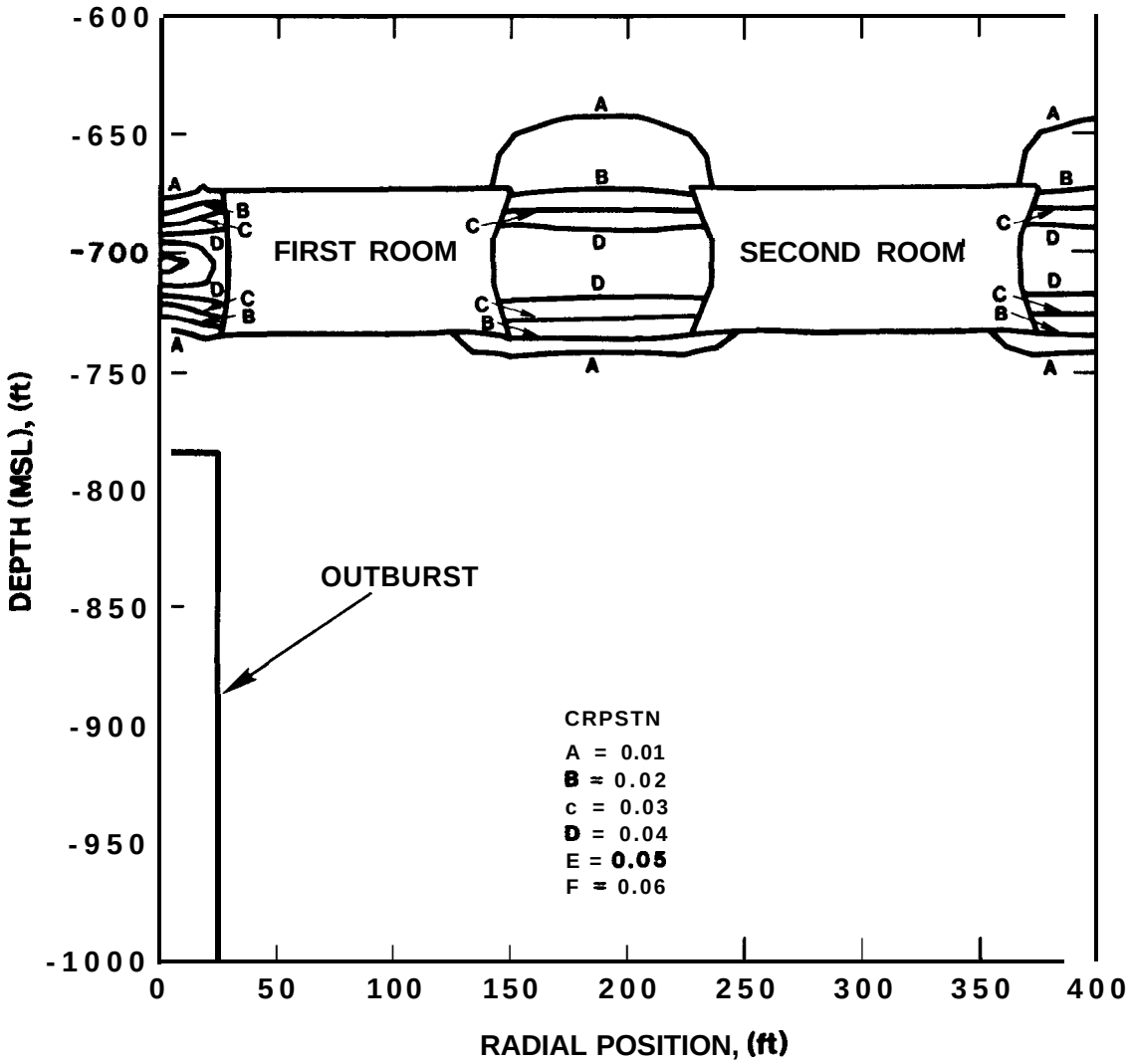


Figure 9. Contours of constant creep strain in the year 2045 assuming an outburst in 1987 due to mining below. The top of the outburst is assumed to be 50 ft beneath a pillar in the SPR.

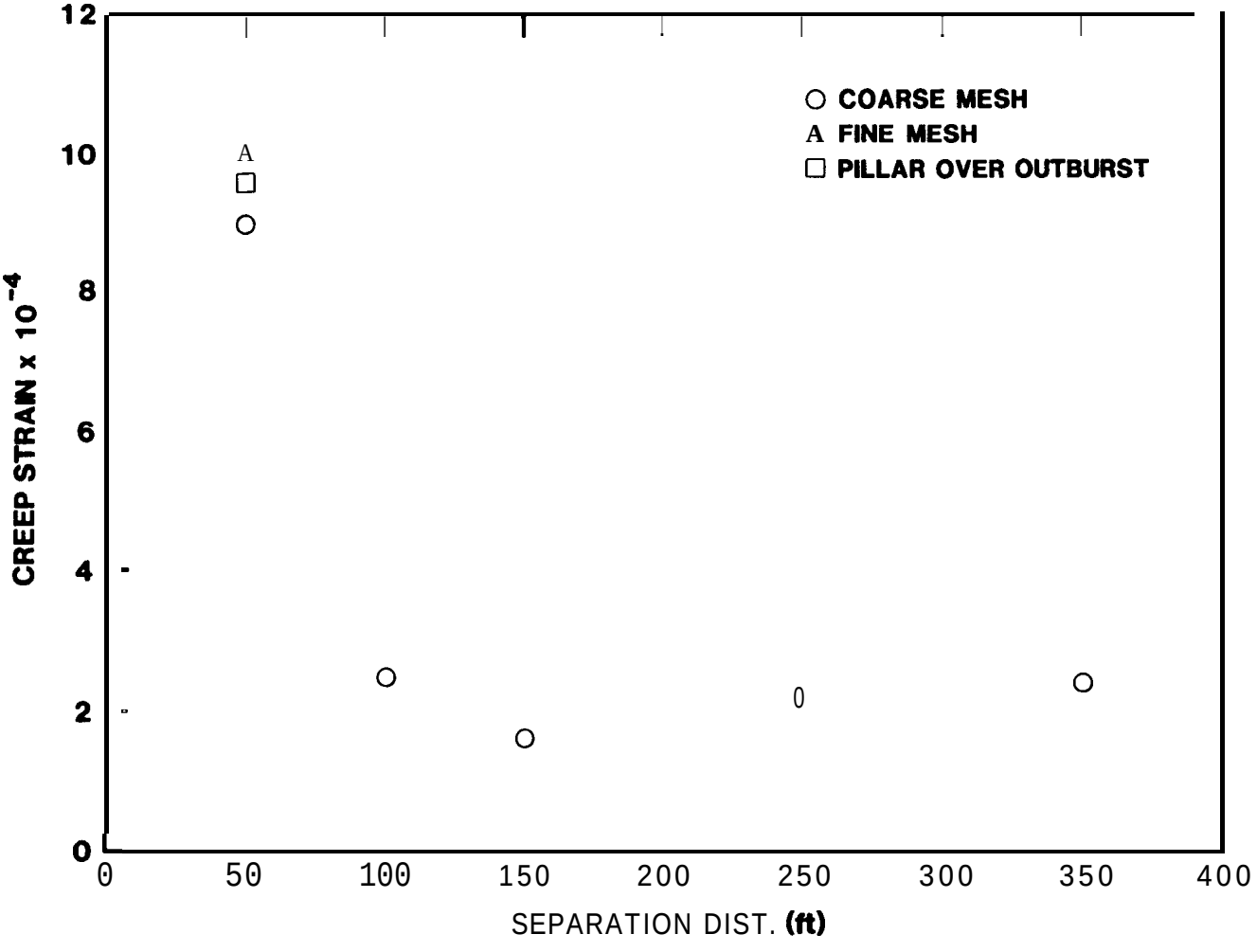


Figure 10. The maximum creep strain in 2045 for all positions on the centerline between the SPR horizon and the top of the postulated outburst, plotted as a function of separation distance between the SPR horizon and the outburst.

## References


1. Ortiz, Terri Smith, "Strategic Petroleum Reserve (SPR) Geological Summary Report Weeks Island Salt Dome," SAND80-1323, Sandia National Laboratories, Albuquerque, NM, October 1980.

2. Henderson, A. J., Jr., "Preliminary Finite Element Study of Proposed Third Level Mine at Weeks Island with Oil Storage in Levels 1 and 2," 1977.

3. Hilton, P. D., S. E. Benzely and M. H. Gubbels, "Structural Analysis of Weeks Island Mine/Petroleum Repository," SAND79-0505, Sandia National Laboratories, Albuquerque, NM, 1979.

4. Key, S. W., C. M. Stone and R. D. Krieg, "A Solution Strategy for the Quasi-Static, Large Deformation, Inelastic Response of Axisymmetric Solids," Proc. of the U.S. - European Workshop on Nonlinear Finite Element Analysis in Structural Mechanics, Ruhr-Univ., Bochum, Fed. Rep. of Ger., July 1980.

5. Key, S. W., C. M. Stone, and R. D. Krieg, "Dynamic Relaxation Applied to the Quasi-Static, Large Deformation, Inelastic Response of Axisymmetric Solids," in Nonlinear Finite Element Analysis in Structural Mechanics, Ed: W. Wunderlich, et al, Springer-Verlag, New York, 1981.

8. Herrmann, W., W. R. Wawersik, and H. S. Lauson, "Creep Curves and Fitting Parameters for Southeastern New Mexico Bedded Salt," SAND80-0087, Sandia National Laboratories, Albuquerque, NM, March 1980.

7. Hansen, F. D., and K. D. Mellegard, "Creep Behavior of Bedded Salt from Southeastern New Mexico at Elevated Temperatures," RSI-0082, RE/SPEC, Inc., Rapid City, SD, November 1977.

8. Herrmann, W., W. R. Wawersik, and H. S. Lauson, "Analysis of Steady State Creep of Southeastern New Mexico Bedded Salt," SAND80-0558, Sandia National Laboratories, Albuquerque, NM, March 1980.

9. Hansen, F. D., "Quasi-Static Strength and Deformational Characteristics of Salt and Other Rock From the Weeks Island Mine," Technical Memorandum Report RSI-0061, RE/SPEC, Inc., Rapid City, SD.

10. Preece, D. S., and J. T. Foley, "Finite Element Analysis of Salt Caverns Employed in the Strategic Petroleum Reserve," Proceedings of the Sixth International Symposium on Salt, Toronto, Ontario, Canada, May 1983.

11. Preece, D. S., and C. M. Stone, "Verification of Finite Element Methods Used to Predict Creep Response of Leached Salt Caverns," Proceedings of 23rd U.S. Symposium on Rock Mechanics, Berkeley, CA, August 1982.

12. Preece, D. S. and W. R. Wawersik, "Leached Salt Cavern Design Using a Fracture Criterion for Rock Salt," Proceedings of 25th Symposium on Rock Mechanics, Northwestern University, June 1984.

13. Krieg, R. D., C. M. Stone, and S. W. Key, "Comparisons of the Structural Behavior of Three Storage Room Designs for the WIPP Project," SAND80-1629, Sandia National Laboratories, Albuquerque, NM, January 1981.

14. Branstetter, L. J., R. D. Krieg, and C. M. Stone, "A Method for Modeling Regional Scale Deformation and Stresses Around Radioactive Waste Deositories in Bedded Salt," SAND81-0237, NUREG/CR-2339, Sandia National Laboratories, Albuquerque, NM, September 1981.

15. Miller, J. D., Stone, C. M., and L. J. Branstetter, "Reference Calculations for Underground Rooms of the WIPP," Sandia National Laboratories, Albuquerque, NM, August 1982.

16. Morgan, H. S., R. D. Krieg and R. V. Matalucci, "Comparative Analysis of Nine Structural Codes Used in the Second WIPP Benchmark Problem," SAND81-1389, Sandia National Laboratories, Albuquerque, NM, November 1981.

17. Wawersik, W. R., W. Herrmann, S. T. Montgomery, and H. S. Lauson, "Excavation Design in Rock Salt – Laboratory Experiments, Material Modeling, and Validations," Proc. of Int'l Symp. on Rock Mech. Related to Caverns and Pressure Shaft." Fed. Rep. of Ger., May 1982.

18. Branstetter, L. J., and D. S. Preece, "Numerical Studies of Laboratory Triaxial Creep Tests," Proceedings of 24th Symposium on Rock Mechanics, Texas A&M University, June 1983.

19. Herrmann, W., and H. S. Lauson, "Analysis of Creep Data for Various Natural Rock Salts," SAND81-2567, Sandia National Laboratories, Albuquerque, NM, December 1981.

20. Price, R. H., W. R. Wawersik, D. W. Hannum, and J. A. Zirzow, "Quasi-Static Rock Mechanics Data for Rock Salt from Three Stategic Petroleum Reserve Domes," SAN81-2521, Sandia National Laboratories, Albuquerque, NM, December 1981.

21. "National Strategic Oil Storage Program, Weeks Island Mine, Geotechnical Study," Vol. 1, Gulf Interstate Engineering Company, Houston, TX, Contract FEA-1251-75.

# APPENDIX A

## Model Description and Detailed Results

## Finite Element Computer Program

SANCHO is a finite element structural computer program developed from HONDO II [4] specifically for predicting creep closure of underground cavities in rock salt [15]. Uses of the program to date are mentioned in the main body of this report and documented in references [10], [11], [12], [13], [14] [15], and [18]. SANCHO is a large strain, large deformation program containing a variety of constitutive models. The solution strategy is based on dynamic relaxation where an "acceleration" term is added to the equilibrium equation converting the static problem into a dynamic one in pseudo-time. An instantaneously "optimum" damping value is computed internally at each time step and used to follow the "transient" response out in pseudo-time until a converged solution is obtained. Satisfaction of global equilibrium at each load step is used to control the convergence of the iterative procedure. The magnitudes of the residual force vector and the applied load vector are compared to determine when global equilibrium has been reached.

The material model for creep is currently restricted to secondary creep expressed in power law form. The creep model is integrated "semi-analytically" which has been shown to be accurate for any strain step size. This method has no stability or time step restrictions as are usually associated with classical Euler integration. The only restriction is that the strain rate should be approximately constant during the time step.

## Material Properties

The salt from Weeks Island has been tested quasi-statically for strength [9] but, to our knowledge, creep tests have never been performed. Even though creep properties vary from site to site it has been shown that the variance from one site to another is usually within the data scatter at any particular site [19]. Thus, the creep model parameters derived from extensive triaxial testing of core from West Hackberry have been used in this study.

As mentioned previously, the program uses a secondary creep model of the form

$$\dot{\bar{e}} = A \exp(-Q/RT)(\bar{\sigma})^n$$

where

$\dot{\bar{e}}$ = secondary effective creep strain rate

A = laboratory determined constant

Q = activation energy

R = universal gas constant

T = temperature, kelvin

$\bar{\sigma}$ = effective stress

n = stress exponent

The coefficients in the above equation have been determined from many months of triaxial creep test data to be

$A = 4.55 \times 10^{-21}$ 1/(day)(psf)$^n$

Q = 13.12 Kcal/(mole K)

n = 4.73

Full treatment of salt creep temperature dependence would require a complete knowledge of the temperature field around the mines. Since data of this type do not exist, the temperature was assumed constant across the mesh and chosen to be the estimated average in the region of interest. In this study the average gas pocket depth ranged from 935 feet to 1235 feet below MSL. Based on this, the temperature at a depth of 1000 feet was used for the entire mesh. This means that the assumed temperature and thus the predicted creep rate on the second level of the mine (-735 feet MSL) are higher than that which actually exists. The temperature at 1000 ft below MSL was estimated to be 90°F in the following manner. The temperature in

the salt at the second level was estimated to be 86°F (based on a measured second level oil temperature of 81°F) and then extrapolated to 90°F at 1000 feet using an estimated gradient of 0.015 F°ft.

The elastic constants used were taken from quasi-static test data on Weeks Island core [9]. The value for Young's modulus is slightly lower than those determined from quasi-static testing of West Hackberry core [20] but the mean values of the moduli from these two sets of data are within the data scatter. The elastic moduli from the two sets of data are given below.

| Data Set | Young's Modulus (psf) | Poisson's Ratio |
|---|---|---|
| West Hackberry | $8.02 \times 10^8$ | 0.30 |
| Weeks Island | $6.38 \times 10^8$ | 0.30 |

## Finite Element Model

The set of intersecting drifts shown in Figure 1 could only be modeled exactly with a three-dimensional finite element program. An economical three-dimensional finite element creep program is not currently available. Even the two-dimensional analyses presented here required roughly 5000 Cpu seconds each on a CRAY 1S. Since the drift configuration had to be analyzed with a two-dimensional program, some approximations had to be made. A previous analysis of this problem [3] treated the drift and gas pocket with a plane strain finite element model. The plane strain assumption treated both the drift and the gas pocket beneath it as infinitely long. This is reasonable for the drift and represents the gas pocket as a worst case since no gas pocket would be of infinite extent. Research since this first analysis has shown the importance of increasing the scope of the model to include more of the dome and whatever underground structures exist [12]. This gives a more accurate prediction of the stress state in the area of interest because interaction with the rest of the dome is included. The best way to accomplish this was to treat the finite element mesh shown in Figure 1 as axisymmetric. The axisymmetric treatment has several advantages: 1)

the gas pocket on the centerline of the mesh is cylindrical and reasonably represents an actual gas pocket and 2) the finite extent of the SPR can be more accurately represented.

The room size on the axisymmetric finite element model was chosen to be larger than a typical room to make the analysis overpredict the displacements and consequently, the strains upon which one of the failure functions is based. The rooms were made 150 ft across in the model compared to a drift size of 40-50 ft in the actual mine. Part of the increase in room size was made to account for the fact that the open space in the mine is created from continuous intersecting drifts which makes rooms larger than just the size of the intersection. The extraction ratio is approximately 65% for the mine [21] and 56% for the finite element model.

The boundary conditions around the edges of the model shown in Figure 3 are modeled as follows. The top of the model (0 depth MSL) represents the ground surface and as such is free to move both vertically and horizontally. The 170 ft of overburden above MSL was not included in all of these analyses, but the assumed lithostatic gradient of 1 psi per foot of depth is slightly higher than actually exists. One analysis was performed with the extra overburden and the difference in the Von Mises stresses and creep strains around the outburst was found to be about 10%. The bottom of the model is prevented from moving vertically but is free to move horizontally. The sides of the model are prevented from moving horizontally but are free to move vertically. The stresses across the model are initialized to lithostatic (1 psi per foot of depth) using gravity loading across the model and lithostatic pressure on the walls of the mine and gas pocket (later to become an outburst). This simulates the stress state in the dome before underground openings were created to disturb the lithostatic stress field. The pressure boundary conditions on the walls of the mine and gas pocket vary with time as follows. Mining of the second level is simulated by linearly reducing the pressure inside the mine from lithostatic to atmospheric over the time from 1955 to 1975. It has been shown that this type of mining simulation is necessary to arrive at the correct stress state [10]. Sudden application of atmospheric pressure inside the mine is equivalent to "shock" loading the model and may give incorrect results.

From 1975 to 1980 the mine remains at atmospheric pressure. Oil fill is simulated from 1980 to 1982 by linearly increasing the pressure from atmospheric to oil head and leaving it constant for the remainder of the analysis. The oil head pressure is computed assuming the free oil surface to be 270 feet below MSL. Lithostatic pressure is maintained inside the gas pocket and reduced suddenly in 1987 to simulate mining into its lower end and creating an outburst. The analysis continues for 58 years beyond this event with oil head pressure in the SPR and atmospheric pressure in the outburst.

The validity of the axisymmetric approximation was verified by comparing the predicted closure of the first, second and third drifts from the centerline of the model shown in Figure 3. In the year 2025, the floor-to-ceiling closure of the first drift is given in Figure 3 to be 28.5 in. The closure of the second and third drifts at the same time was 28.1 inches and 27.8 inches. The fact that the closure predictions for all three drifts are similar indicates that the model is a reasonable simulation of the rectangular array of parallel drifts in the SPR lower level.

Seven different analyses were completed using the finite element model and the history just described. These analyses are summarized in Table Al. In the first five analyses the separation distance between the SPR level and the top of the gas pocket was varied from 350 feet to 50 feet. These models are shown in Figures Al through A5. The sixth analysis treated a 50 foot separation distance with the mesh refined in the region between the mine and gas pocket as shown in Figure A8. This was done to ensure that the mesh was fine enough in analyses 1 through 5. No significant changes in the results were noted between the coarse mesh (Figure A5) and the fine mesh (Figure A6). The seventh analysis included a pillar immediately above the gas pocket since an outburst is just as possible beneath a pillar as beneath the center of a room. This pillar was modeled as 50 feet in diameter, the same as the gas pocket, and approximately the same size as a 40 X 40 foot pillar existing in the SPR. This model is shown in Figure A7.

Potential failure of the web between the mine and the outburst was assessed using two failure models that treat different failure mechanisms.

The first was a simple Mohr-Coulomb failure envelope derived from quasi-static triaxial tests of Weeks Island core [9] and is given as

$$\tau = T_s + \sigma \tan \phi$$

where

$\tau$ = Shear stress on the failure plane.

$T_s$ = Tensile strength = 330 psi.

$\sigma$ = Normal stress on the failure plane.

$\phi$ = Friction angle = 56 degrees.

This equation was included in a failure criterion that could be calculated from the finite element results (stresses) at each time step and at each element. The failure criterion took the following form

$$\text{Mohrf} = \tau_{max} - T_s - (\phi)\tan(\sigma_{max} + \sigma_{min})/2.0$$

where

Mohrf = Failure function value (positive for failure).

$\tau_{max}$ = Maximum predicted shear stress.

$\sigma_{max}$ = Maximum predicted principal stress.

$\sigma_{min}$ = Minimum predicted principal stress.

In using this failure criterion it must be remembered that the shear stresses around the gas pocket resulting from sudden pressure reduction are dissipated with time through creep. A Mohr-Coulomb failure will occur almost immediately after the outburst occurs, if at all, since this is the time of maximum shear stress. Figures A8 and A9 show contour plots of the Mohr failure function ixnediately after the outburst occurrence. These two figures show that Mohr-Coulomb type failures are unlikely for a web thickness of 50 feet.

Another mechanism of rock salt failure results from damage to the salt structure due to excessive creep strain. A creep failure criterion has been developed from laboratory triaxial creep and quasi-static tests [12]. This failure criterion is a function of confining pressure and creep strain and has the following form

$$\text{Creepf} = 100.0(\varepsilon_c - 0.023 - f(P))$$

$$f(P) = P\,(2.117 \times 10^{-6} - P\,(8.450 \times 10^{-12}))$$

where

Creepf = Creep failure function (positive for failure).

$\varepsilon_c$ = Effective creep strain.

P = Confining pressure = $(\sigma_1 + \sigma_2 + \sigma_3)/3.0$

The results from the finite element analyses (stresses and strains) for each time step and each element have been processed to give values of the creep failure function that can be examined for failure potential. Since this failure function is dependent on creep strain, the potential for failure increases with time as more creep strain is accumulated. Figures A10 and All show contour plots of the creep failure function 58 years after the gas pocket outburst . The outburst region is assumed to be unreinforced during this time. The figures indicate that failure due to excessive creep strain is unlikely. This is also logical since the SPR horizons are relatively shallow and one would not expect to see excessive creep strains.

The final method used to assess a safe separation distance was the determination of over 1 apping zones of influence of the drift and the outburst gas pocket. The two parameters used to determine the separation distance at which the influence zones overlap were Von Mises stress and creep strain. Graphs of separation distance versus maximum Von Mises stress and separation distance versus maximum creep strain are found in the main body of this report in Figures 7 and 10. These figures indicate that the drift and the outburst gas pocket do not influence each other until the separation distance is 50 feet. Even at this distance the overlapping of influence zones is relatively minor.

Table A1. Summary of Finite Element Analyses

| Analysis No. | Mine to Outburst (Ft ) | Notes |
|---|---|---|
| 1 | 350 | Course Mesh |
| 2 | 250 | " |
| 3 | 150 | " |
| 4 | 100 | " |
| 5 | 50 | " |
| 6 | 50 | Mesh refined between mine and outburst |
| 7 | 50 | Pillar over outburst |

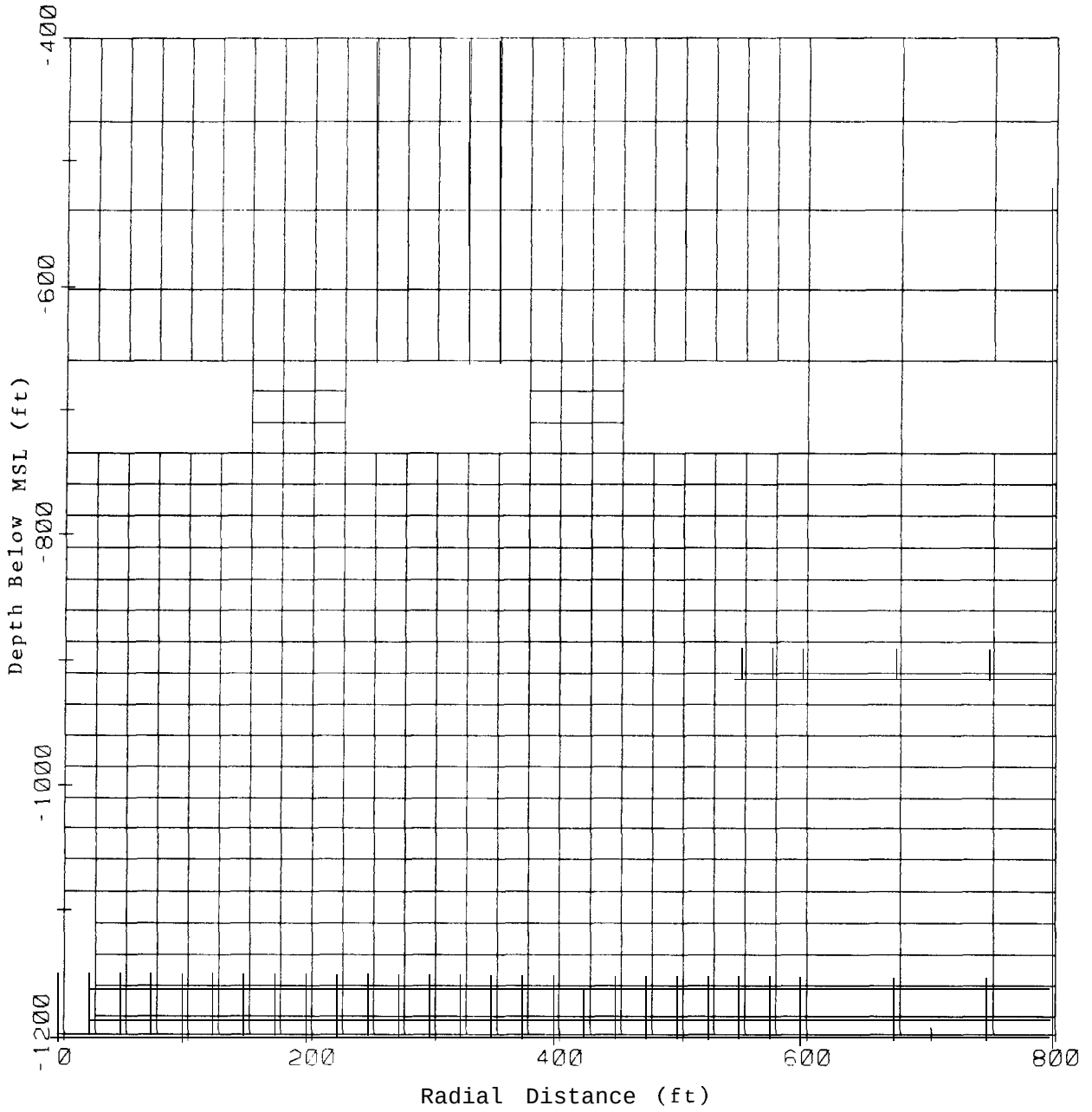


Figure A1. Axisymmetric Finite Element Mesh for a Mine to Outburst Separation Distance of 350 ft.

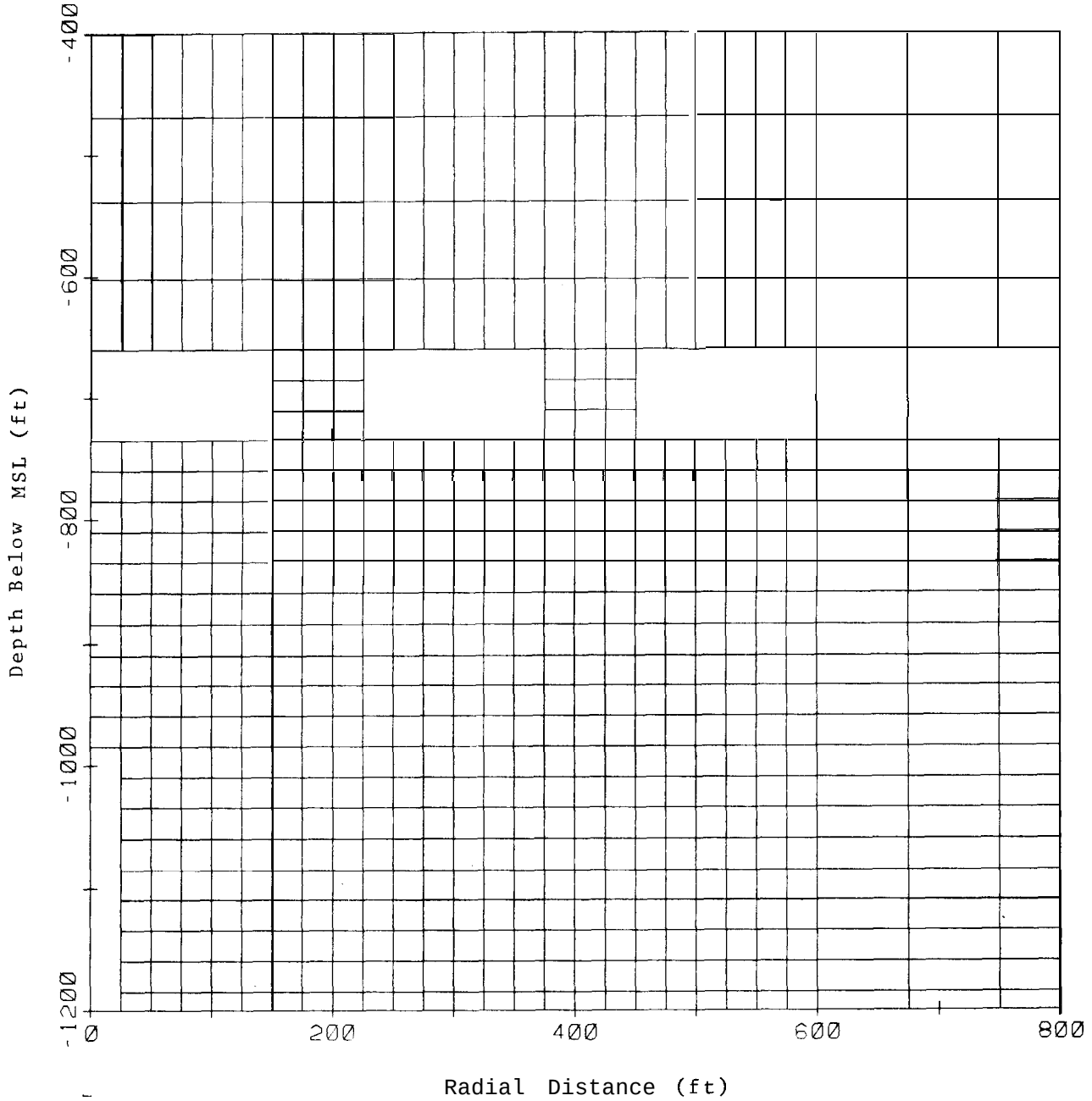


Figure A2. Axisymmetric Finite Element Mesh for a Mine to Outburst Separation Distance of 250 ft.

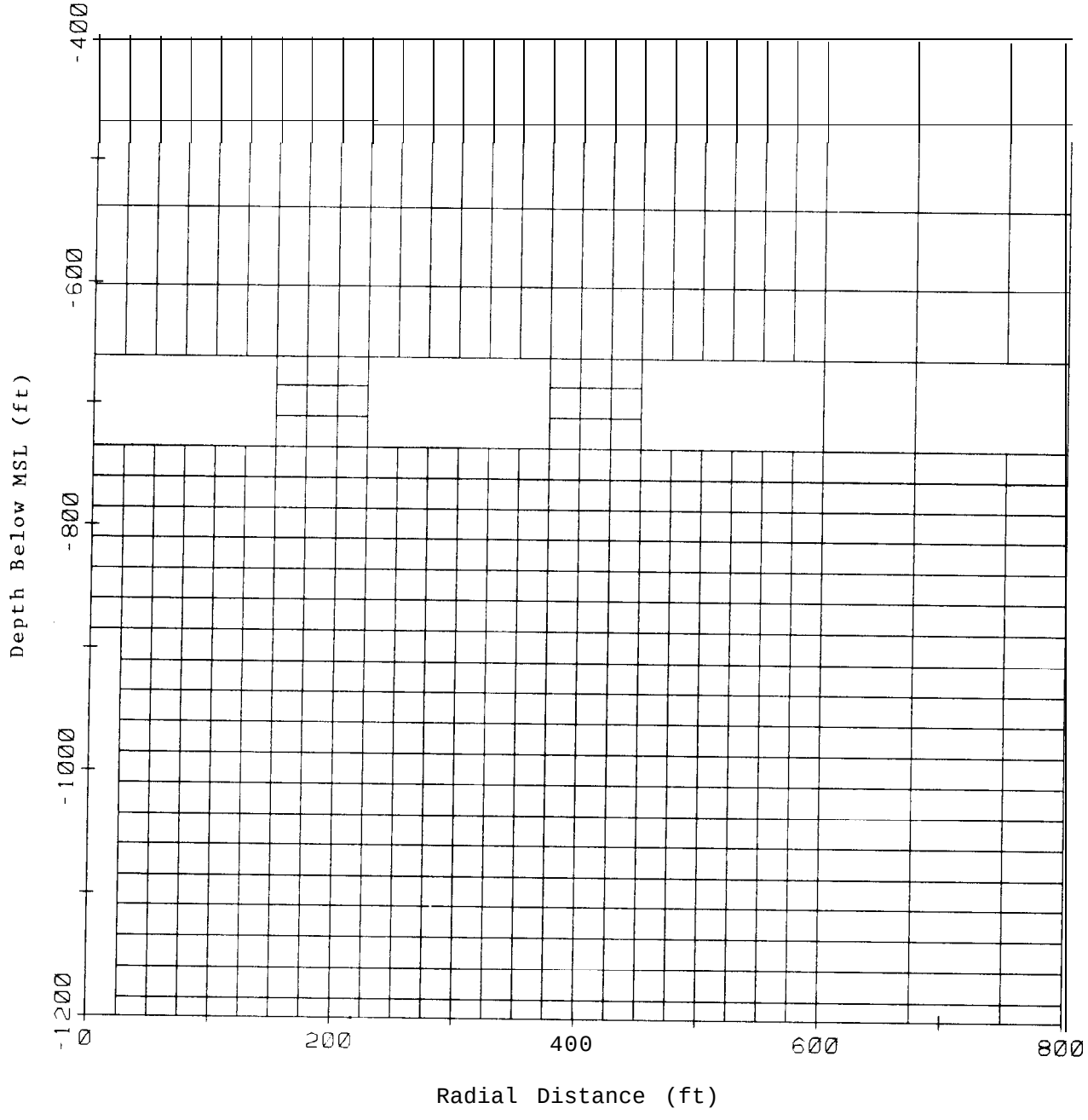


Figure A3. Axisymmetric Finite Element Mesh for a Mine to Outburst Separation Distance of 150 ft.

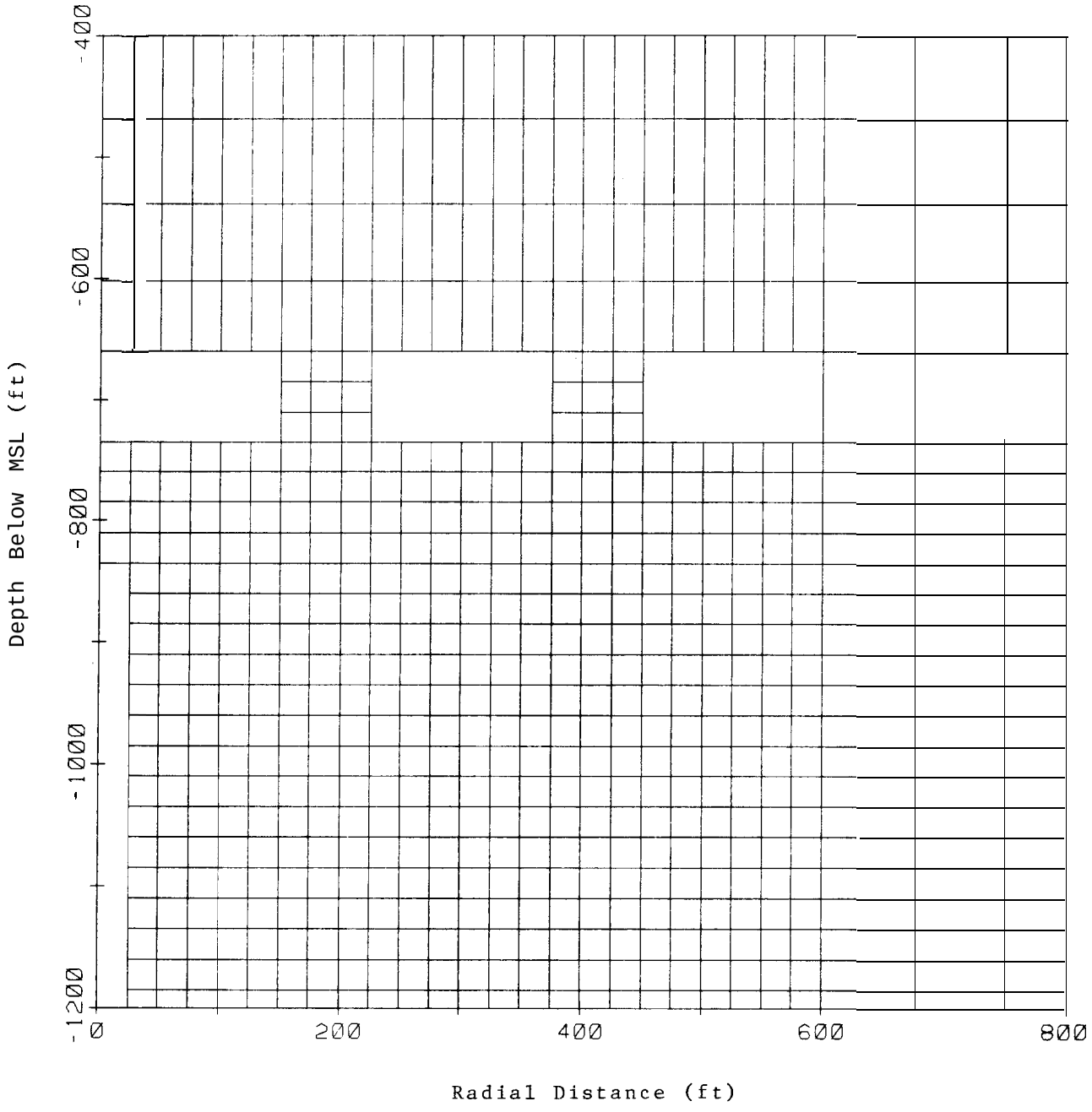


Figure A4. Axisymmetric Finite Element Mesh for a Mine to Outburst Separation Distance of 100 ft.

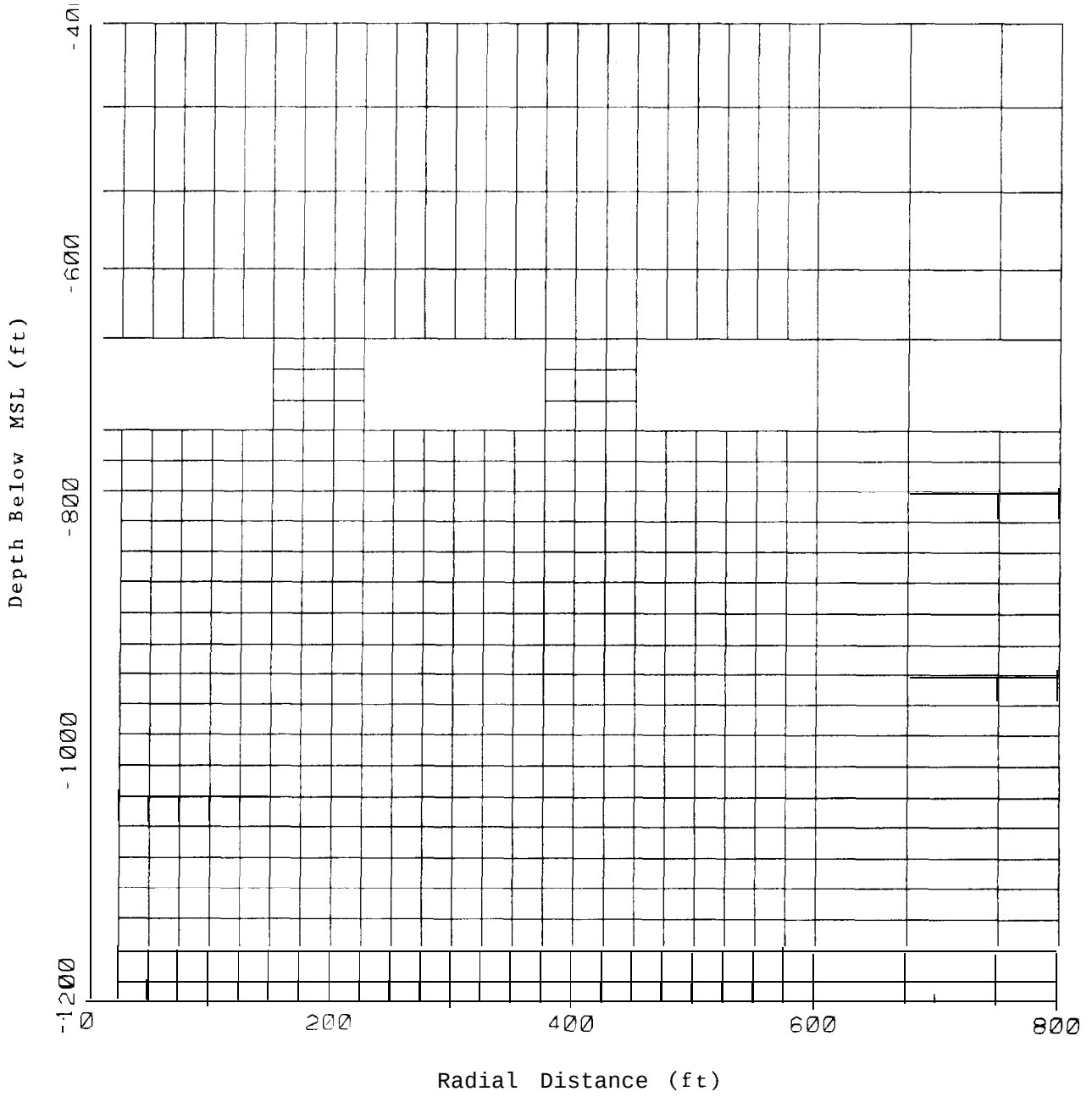


Figure A5. Axisymmetric Finite Element Mesh for a Mine to Outburst Separation Distance of 50 ft.

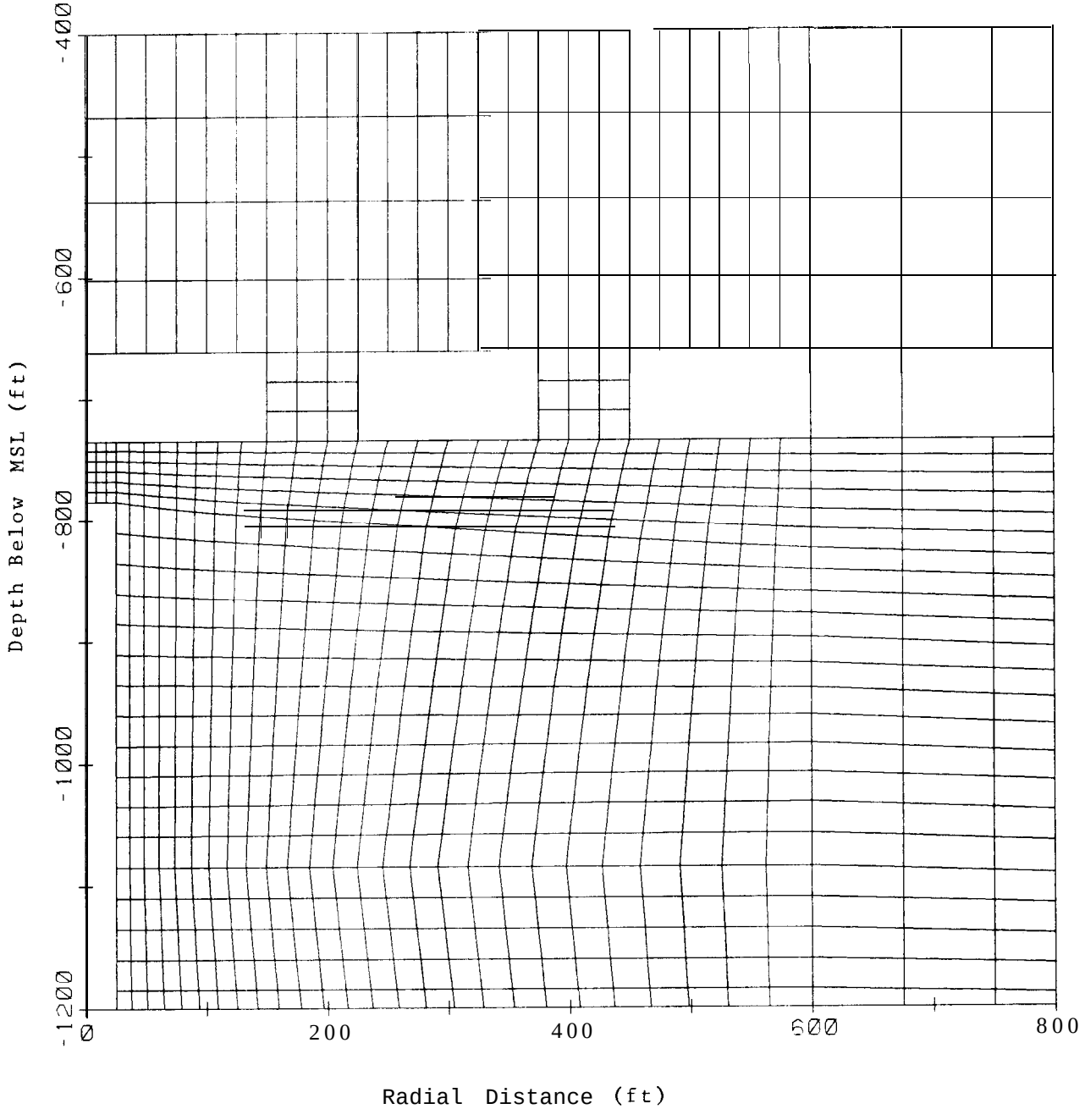


Figure A6. Axisymmetric Finite Element Mesh for a Mine to Outburst Separation Distance of 50 ft with More Elements in the Roof Region.

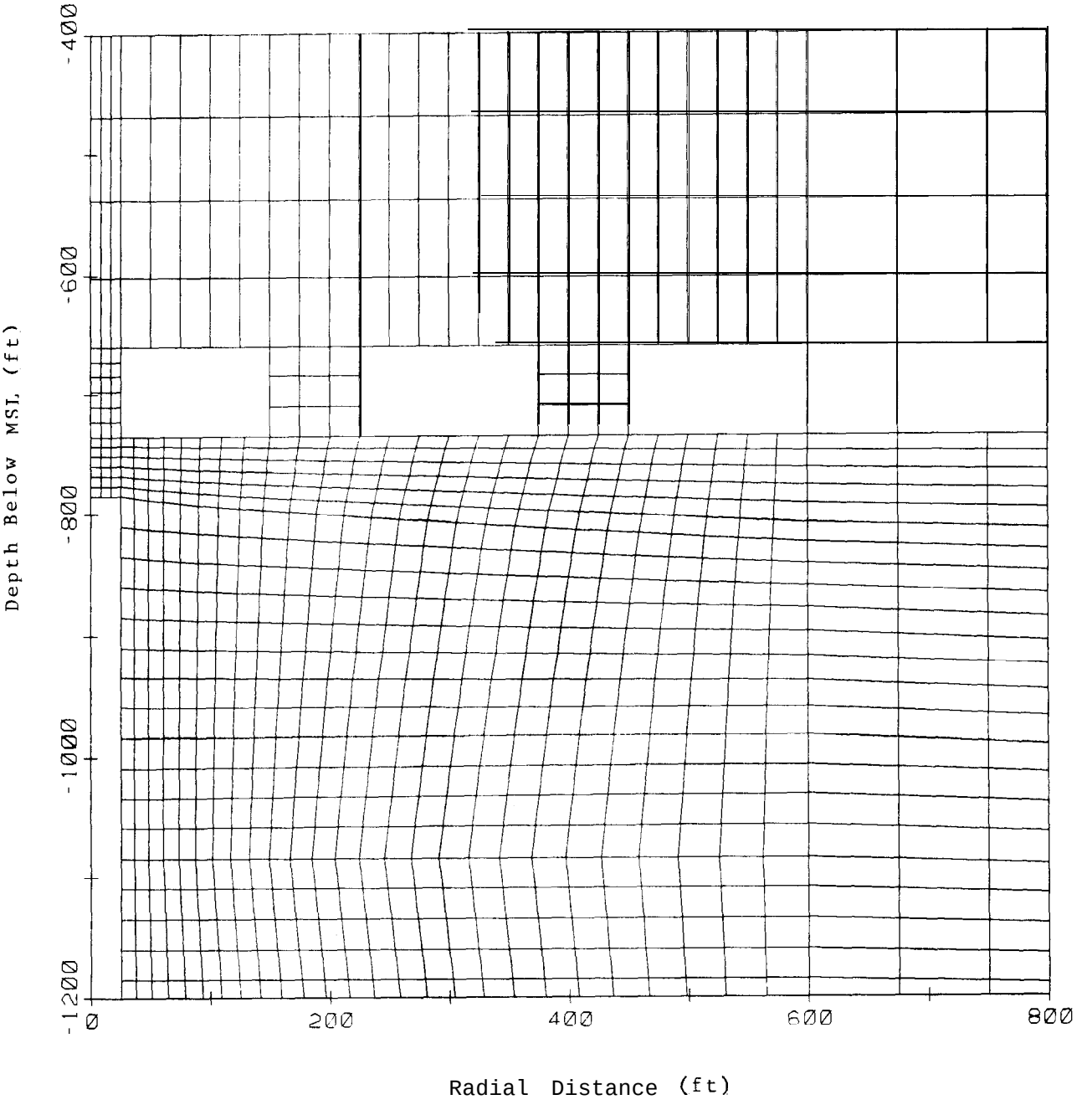


Figure A7. Axisymmetric Finite Element Mesh for a Mine to Outburst Separation Distance of 50 ft with a Pillar Immediately Above the Outburst.

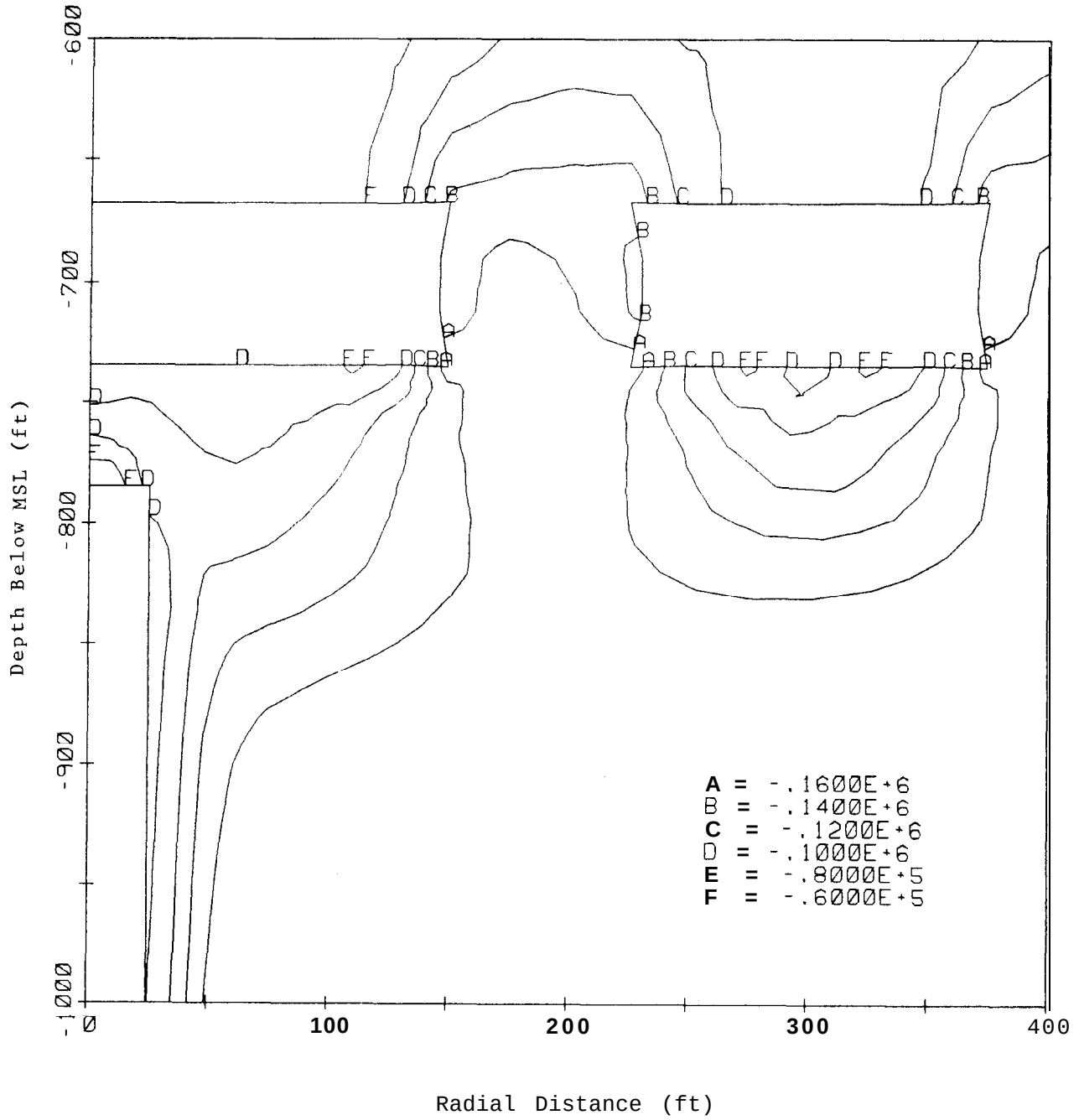


Figure A8. Contours of the Mohr Failure Function (Positive Indicates Failure) Immediately After Outburst Occurrence Beneath the Center of a Room.

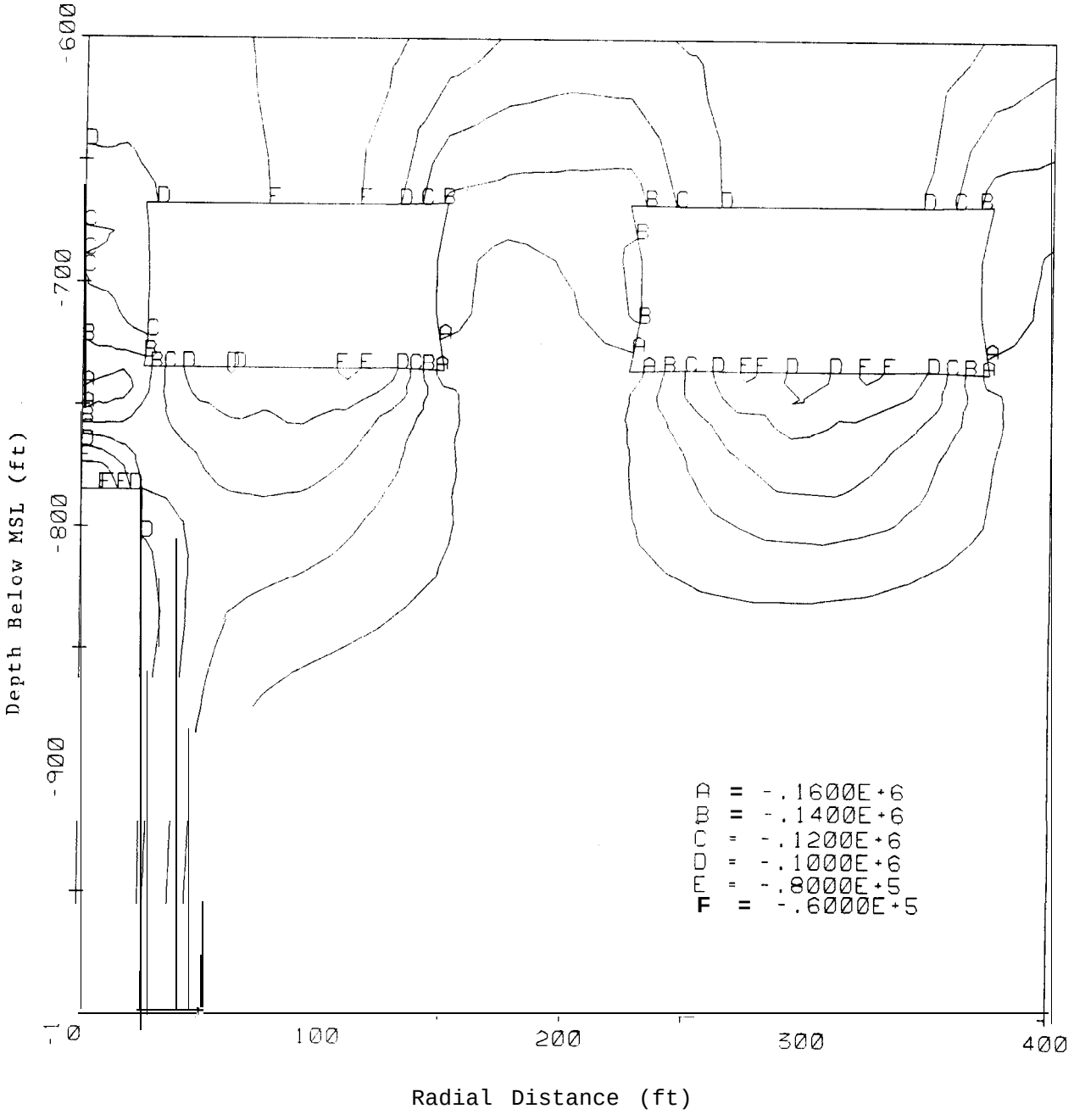


Figure A9. Contours of the Mohr Failure Function (Positive Indicates Failure) Immediately After Outburst Occurrence Beneath a Pillar.

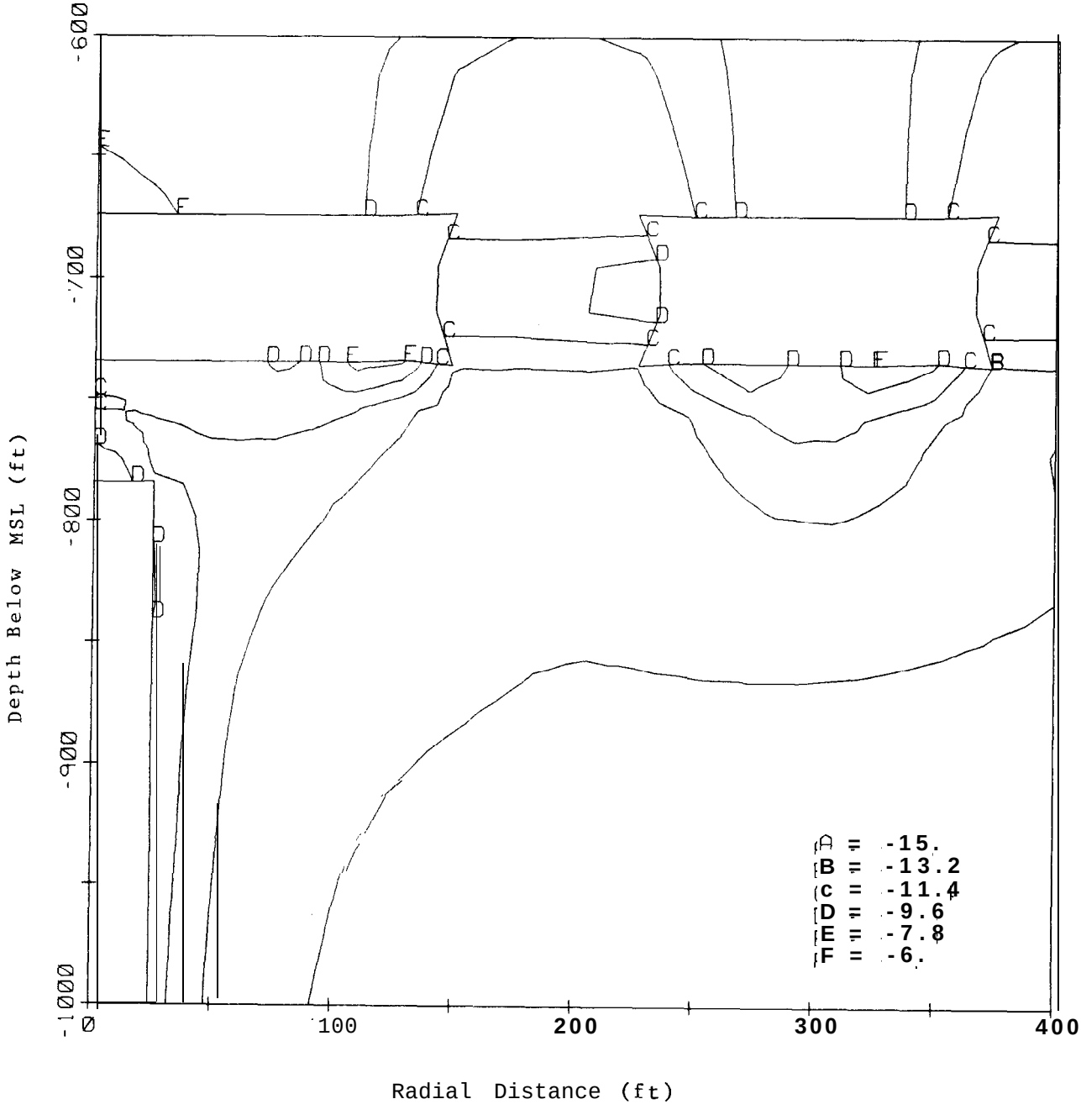


Figure A10. Contours of the Creep Strain Failure Function (Positive Indicates Failure) 60 Years After Outburst Occurrence Beneath the Center of a Room.

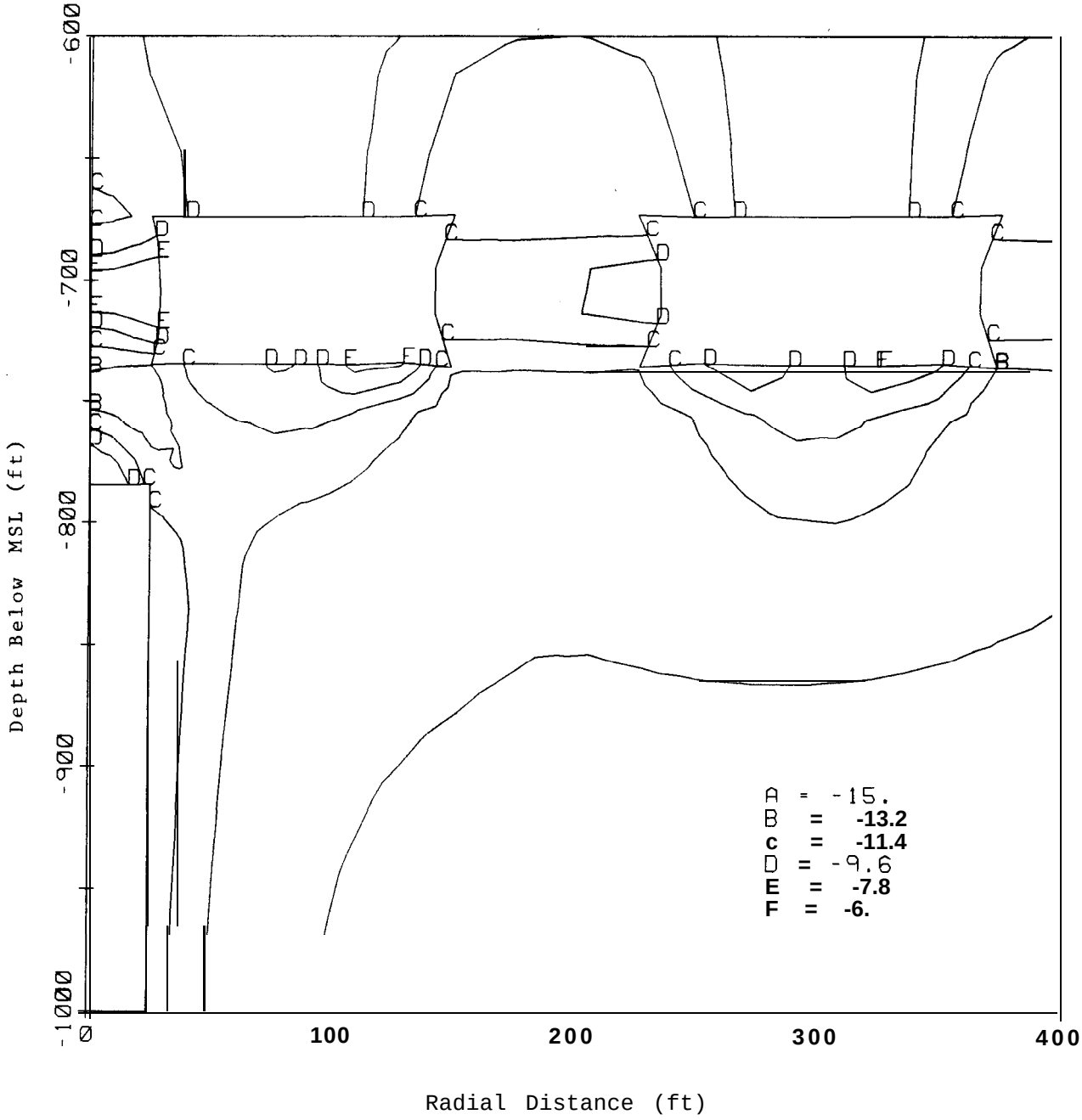


Figure All. Contours of the Creep Strain Failure Function (Positive Indicates Failure) 60 Years After Outburst Occurrence Beneath a Pillar.

# APPENDIX B

## Definitions and Discussion of Stress and Strain Measures

The conclusions in the body of the paper are predicated on plots of various stress and strain measures. It is necessary to have at least an intuitive understanding of these terms in order to comprehend what is being stated.

Stress and strain are very rigorously defined abstract quantities which require a mathematical background in tensor analysis to understand in full detail. Those definitions are used extensively in finite element programs and SANCHO in particular. However, it is not necessary to be abstract to understand the fundamental ideas involved.

Stress is a measure related to forces and strain is related to distortion. Consider a long circular 0.2 inch diameter rod which we suspend by one end. On the other end, we hang a 1000 lb weight. Thus, the average normal stress on the rod is 31,800 psi (pounds per square inch). This is computed by dividing the 1000 lb force by the area ($\pi r^2$) through a cross section, 0.0314 square inches (3.141 x 0.2 x 0.2/4) of the rod. If we had marked a pair of points on the rod 0.3 inches apart prior to attaching the weight, then the stretch in the rod would be noted by the distance the points moved apart. If this stretch or displacement is 0.0032 inches, then the average normal strain in the rod is 0.00107 in/in (inches per inch). This is found by dividing the 0.0032 in displacement by the original 0.3 inch separation between the points.

The concept of stress and strain are particularly useful since they are generalized quantities, i.e., concerned with the conditions at any point rather than conditions in a particular sized bar. All particles in the uniform bar, both inside and on the surface, are experiencing a 31,800 psi stress and a 0.00107 in/in strain. Since material properties tests are ordinarily made at least conceptually with the geometry of a rod, we often relate conditions back to the rod.

Another valuable concept is that of shear. Shear stress and shear strain are measures of distortional processes. This is illustrated, for example, by gluing a 0.2 inch tall block to the floor, applying a 1000 lb force to the top of the block in a direction parallel to the floor and

measuring the forward movement of the top face with respect to the base. If a 0.0004 inch displacement is measured, the shear strain is calculated to be 0.0004 divided by 0.2 or 0.002 in/in. The shear stress for this problem can be found if we know the block has a 0.2 in by 0.2 in base (or 0.04 square inch cross sectional area). The shear stress is 25,000 psi or 1000 lb divided by 0.04 sq. in. Note again that shear stresses and shear strains are generalized quantities describing conditions at a point.

Volumetric strain measures volume change under an imposed pressure. It is computed by dividing the change by the original volume.

We see that the state of stress and strain at a particle are not simple quantities. For example, the cube described above could have different shear forces applied to each pair of faces. A particle in the cube would then have three different shear stresses and three different shear strains associated with it. In any non-trivial structural problem, the particles are in complex three-dimensional states of stress and strain. We are concerned in the SPR problem about creep of the salt and the stresses which cause it.

It has been found that under a pure state of pressure, i.e., with no shear stresses imposed, materials will not creep. This is true of rock salt also. Since creep is the most interesting phenomenon in the SPR, we consider combinations of stress and strain which measure creep or tendency to (stresses which cause) creep. The effective creep strain and the effective (or Von Mises) stress are such measures. These are non-directional quantities which are independent of volume change and pressure, respectively.

Generally, any set of stresses acting on a particle which has the same Von Mises stress as another set of (different) stresses will produce a set of creep strains (different from the first set) which has the same or nearly the same effective creep strain as the other.

The effective stress and effective creep strain have been cleverly defined such that they are identical to the normal stress and normal strain in a long rod. For example, consider a normal stress of 5000 psi in a long

rod which produces a normal strain which increases at a rate of 0.001 in/in in a day. Then a structure of the same material with a complex set of loads will have almost all points in a complex state of strain which are also increasing. A point with a Von Mises stress of 5000 psi, however, will have a complex state of straining which has an effective creep strain rate of 0.001 in/in per day. The stress and creep strain states in a sense "effectively" have the same relation as if they were in a long rod of the same material.

Distribution:
U.S. DOE
Oak Ridge Operations Office
P. 0. Box E
Oak Ridge, TN 37831
Attn: P. Brewington, Jr.

Jocelyn Guarisco, General Counsel (15)
DOE SPR PMO, OGC
900 Commerce Road East
New Orleans, LA 70123

Land Acquisition Section (2)
Land and Resource Division
Department of Justice
9th and Penn. Ave., N.E.
Washington, DC 20530
Attn: Donald Rosendorf, Attorney
Gerold T. Levin, Attorney

Madelyn R. Creedon
Headquarter, DOE
Mail Stop GC-23, 6H-087
Washington, DC 20585

DOE SPR
P. 0. Box 434
New Iberia, LA 70569
Attn: E. Thiele

DOE SPR PMO
900 Commerce Road East
New Orleans, LA 70123
Attn: R. Somerlock PR-61
E. Chaple PR-632 (3)
L. Rousseau PR-632

Dr. Steve Benzley
Civil Engineering, 368CB
Brigham Young University
Provo, UT 84602

Dr. Peter D. Hilton
Arthur D. Little, Inc.
Acorn Park
Cambridge, MA 02140

0400 J. F. Ney
1510 J. W. Nunziato
1520 D. J. McCloskey
1521 R. D. Krieg (5)
1521 H. S. Morgan
1521 D. S. Preece (20)
1524 L. J. Branstetter
1530 I,. W. Davison
1540 W. C. Luth
1542 B. M. Butcher
1542 W. R. Wawersik
2312 M. H. Gubbles
6200 v. L. Dugan
6240 R. K. Traeger
6250 B. W. Marshall
6253 D. A. Northrop
6257 J. K. Linn (5)
6257 R. R. Beasley
6257 D. K. Buchanan
6257 T. L. Todd, Jr
6310 T. 0. Hunter
6312 F. W. Bingham
Attn: T. S. Ortiz
6313 J. R. Tillerson
6330 W. D. Weart
6331 A . R. Lappin
6332 L. D. Tyler
6430 N. R. Ortiz
8120 L. D. Berthoff
8310 R. W. Rohde
3141 C. M. Ostrander (5)
3151 W. L. Garner (3)
3154-2 C. H. Dalin (25)
(Unlimited Release for DOE/TIC)
8424 M. A. Pound